Journal of Physiology (1991), **440**, *pp.* 659–696
With 18 *figures*
Printed in Great Britain

AN INTRACELLULAR ANALYSIS OF THE VISUAL RESPONSES OF NEURONES IN CAT VISUAL CORTEX

BY RODNEY J. DOUGLAS*†, KEVAN A. C. MARTIN* AND DAVID WHITTERIDGE*

*From the *MRC Anatomical Neuropharmacology Unit, Department of Pharmacology, South Parks Road, Oxford OX1 3QT and the †Department of Physiology, University of Cape Town Medical School, Observatory 7925, Cape Town, South Africa*

(*Received 6 March 1990*)

SUMMARY

1. Extracellular and intracellular recordings were made from neurones in the visual cortex of the cat in order to compare the subthreshold membrane potentials, reflecting the input to the neurone, with the output from the neurone seen as action potentials.

2. Moving bars and edges, generated under computer control, were used to stimulate the neurones. The membrane potential was digitized and averaged for a number of trials after stripping the action potentials. Comparison of extracellular and intracellular discharge patterns indicated that the intracellular impalement did not alter the neurones' properties. Input resistance of the neurone altered little during stable intracellular recordings (30 min–2 h 50 min).

3. Intracellular recordings showed two distinct patterns of membrane potential changes during optimal visual stimulation. The patterns corresponded closely to the division of S-type (simple) and C-type (complex) receptive fields. Simple cells had a complex pattern of membrane potential fluctuations, involving depolarizations alternating with hyperpolarizations. Complex cells had a simple single sustained plateau of depolarization that was often followed but not preceded by a hyperpolarization. In both simple and complex cells the depolarizations led to action potential discharges. The hyperpolarizations were associated with inhibition of action potential discharge.

4. Stimulating simple cells with non-optimal directions of motion produced little or no hyperpolarization of the membrane in most cases, despite a lack of action potential output. Directional complex cells always produced a single plateau of depolarization leading to action potential discharge in both the optimal and non-optimal directions of motion. The directionality could not be predicted on the basis of the position of the hyperpolarizing inhibitory potentials found in the optimal direction.

5. Stimulation of simple cells with non-optimal orientations occasionally produced slight hyperpolarizations and inhibition of action potential discharge. Complex cells, which had broader orientation tuning than simple cells, could show marked hyperpolarization for non-optimal orientations, but this was not generally the case.

MS 8325

6. The data do not support models of directionality and orientation that rely solely on strong inhibitory mechanisms to produce stimulus selectivity.

INTRODUCTION

The past decade has seen major advances in our understanding of the microcircuitry of the cerebral cortex (see reviews: Gilbert, 1983; Lund, 1988; Martin, 1988; White, 1989; Douglas & Martin, 1990), but the functional operations of the local circuits remain poorly understood. This state of affairs is in part due to technical reasons: intracellular recording is the only technique that permits a direct view of the subthreshold synaptic potentials that produce inhibition or excitation. Although heroic efforts have been made (e.g. Dreifuss, Kelly & Krnjević, 1969; Creutzfeldt, Kuhnt & Benevento, 1974; Ferster & Lindström, 1983; Ferster, 1986), the extreme difficulty of obtaining intracellular recordings *in vivo*, together with the problems of interpreting the records (see Martin, 1988), has meant that intracellular recording in neocortical neurones has been largely restricted to *in vitro* slice preparations where the experimental options are severely limited, if only because much of the circuitry has been stripped away. As a result, the program to analyse the functions of local cortical circuits *in vivo* has had to use relatively indirect methods to analyse the synaptic events underlying the responses of cortical neurones.

Since the first studies by Hubel & Wiesel (1959, 1962) it has been evident that the structure of cortical receptive fields might be determined by an interaction of inhibitory and excitatory processes. Through the use of multiple stimuli (e.g. Bishop, Coombs & Henry, 1971; Movshon, Thompson & Tolhurst, 1978*a*, *b*; Heggelund, 1981*a*, *b*; Ganz & Felder, 1984) or various pharmacological techniques (e.g. Hess & Murata, 1974; Sillito, 1975; Bolz & Gilbert, 1986; Ramoa, Shadlen, Skottun & Freeman, 1986) evidence has accumulated that the selective properties of cortical neurones (orientation, directionality, end-inhibition, subfield antagonism) arise as a result of postsynaptic inhibitory processes that shape a relatively unselective excitatory input from the thalamus. In order to explain the tuning of the action potential discharge, inferences have been made as to the pattern of postsynaptic inhibitory potentials (e.g. Movshon *et al.* 1978*a*; Palmer & Davis, 1981*a*, *b*; see Orban, 1984). However, the inferences about the underlying synaptic events that are obtained from extracellular recording are necessarily indirect and may be misleading, as Ferster (1986) has argued for the case of orientation selectivity.

In this first of a series of four papers, we use a combination of extracellular and intracellular recording in the whole animal to describe the relationship of the subthreshold postsynaptic potentials to the presence or absence of action potential discharge. We anticipated that inhibition would be clearly revealed in three particular situations: between the subfields of simple cells, in direction selectivity, and in orientation selectivity. When we tested these aspects, however, we were struck by the fact that the most pronounced hyperpolarizing (inhibitory) potentials were evoked by *optimal* stimuli. Non-optimal stimuli did not evoke the strong hyperpolarizing potentials traditionally associated with inhibition. The remaining three papers are concerned with our attempt to understand why this is so.

In the second paper we investigate the mechanisms of intracortical inhibition. We confirm, using intracellular recording, that postsynaptic inhibition is indeed present

in cortical neurones. We found that the amplitude of the membrane hyperpolarizations associated with the visually evoked inhibition of action potential discharge is small (< 5 mV). One explanation for this observation is that the inhibitory currents are due to large changes in membrane conductance that 'shunt' excitatory current, rather than to small conductance changes coupled with large membrane hyperpolarizations. However, we found that the suppression of action potential discharge during periods of presumed inhibition was not accompanied by the large conductance change that would indicate the presence of shunting inhibition.

We considered the possibility that we did not detect a significant component of intracortical inhibition because the inhibitory synapses were located at electrotonically distant sites like dendritic spines. In such a situation their effects would not be readily visible from recordings made in the soma (see Koch, Douglas & Wehmeier, 1990). In paper three we discount this possibility by using anatomical methods to show that dendritic spines receiving synapses from afferents of the lateral geniculate nucleus rarely receive an additional putative inhibitory synapse.

Thus, we are left with the conundrum that extracellular studies show ample evidence of inhibitory processes, but intracellular recording reveals remarkably little of this inhibition. Therefore, in the fourth paper we examine the interaction of the excitatory and inhibitory events that follow simple pulse activation of the cortex. We develop and test a hypothesis of the organization and function of the cortical microcircuitry that resolves the conundrum and offers a novel explanation of the generation of the selective properties of cortical neurones.

METHODS

The basic methods for these experiments have been given in detail in Martin & Whitteridge (1984).

Preparation and maintenance of animals

Twenty-seven cats (2·3–3·0 kg body weight) were anaesthetized with an oxygen–halothane–nitrous oxide mixture. The femoral artery and vein were cannulated, halothane was discontinued and anaesthesia and analgesia were maintained with alphaxalone–alphadolone (Saffan, Glazo) and 70% nitrous oxide–30% oxygen. A tracheotomy was performed and the cat was paralysed with gallamine triethiodide (80 mg induction dose, 13 mg kg^{-1} h^{-1} thereafter) and tubocurarine (1 mg kg^{-1} h^{-1}). The cat was artificially respired with the nitrous oxide–oxygen mixture. The Saffan was discontinued and anaesthesia was maintained with sodium barbiturate (2–3 mg kg^{-1} h^{-1}) except for a few experiments where Saffan was used throughout. The end-tidal P_{CO_2} was monitored continuously and maintained between 4·5 and 5·0%. The rectal temperature, blood pressure, heart rate and electroencephalogram (EEG) were also continuously monitored and were used together to determine the anaesthetic level. Neutral contact lenses were placed over the cornea and appropriate correction lenses were placed in front of the eyes to focus them on the tangent screen or oscilloscope, 1·14 m away.

Stimulating electrodes

Pairs of varnished tungsten stimulating electrodes were inserted in the optic chiasm (OX), the optic radiations (OR) immediately above the lateral geniculate nucleus (site OR1), the radiations immediately below the cortex (site OR2), and in the radiations beneath the visual cortex of the opposite hemisphere. Visually evoked potentials were recorded through the stimulating electrodes to ensure their correct placement. The latency of response of the recorded neurones to stimulation at these various positions provides important information as to their input (Hoffman & Stone, 1971; Bullier & Henry, 1979; Henry, Harvey & Lund, 1979; Ferster & Lindström, 1983; Martin & Whitteridge, 1984).

Recording pipettes

The micropipettes were filled with a 4% solution of horseradish peroxidase (HRP) in a 0·2 M-KCl solution buffered with 0·05 M-Tris, pH 7·9. This was ejected with positive current pulses ranging from 2 to 4 nA. The pipettes were bevelled to 100 MΩ. In some experiments unbevelled electrodes filled with 3 M-KCl or 2 M-potassium citrate were used. The results obtained with these were not different from those of the horseradish peroxidase electrodes. A plastic cylinder was placed around the craniotomy (over the postlateral gyrus at Horsely–Clarke AP co-ordinates −3 to −6 mm), which was filled with agar and topped with paraffin wax after the pipette had been placed in position above the cortex. A stepper motor advanced the pipette in 2 μm steps until an extracellular response was recorded.

Electronics

Intracellular recordings were made with a Neurolog NL102 preamplifier (Digitimer) and in some cases an Axoclamp 2A preamplifier (Axon Instruments, Burlingame, CA, USA). The microelectrode voltage and current were logged by a CED1401 (Cambridge Electronic Design) intelligent interface. The CED1401 also controlled intracellular current injection, and extracellular stimulation.

The microelectrode voltage signal was filtered (24 dB or 48 dB octave^{-1} Butterworth, frequency = 0·5–0·7 kHz, Kemo VBF/3) before being digitized (12 bit) at 2 kHz. In these experiments we were particularly interested in membrane voltage fluctuations beneath the threshold for action potential generation, and the correlation of these events with visual stimulation. In order to maintain good resolution the amplification and offset were continually adjusted to optimize the peak-to-peak amplitude of the signal with respect to the range of the analog-to-digital converter. Typically the signal occupied 50% of the range.

Standard intracellular recording methods were used. It should be noted that we spent between 15 and 60 min in the extracellular space outside the cell before penetration. During this time the receptive field was hand-plotted, latencies to optic radiation stimulation were measured, and the receptive field properties were quantified using peristimulus time histograms of action potential discharge. In addition, the DC offset, capacitance compensation, and bridge balance were trimmed. Once inside the cell, the balance and capacitance compensation were checked using a biphasic rectangular current pulse. If possible, further trimming of the amplifier was avoided until the pipette was withdrawn from the cell. Where necessary the bridge was rebalanced inside the neurone so that the charging of the membrane capacitance at the onset of the current began smoothly from the resting potential (Purves, 1981). Thereafter extracellular controls were performed.

Sometimes premature impalement of the cell began to occur during extracellular recording. Attempts to trim the amplifier again risked injuring the neurone. Under these circumstances we ignored capacitance compensation unless the error was severe, and used biphasic rectangular injection current to balance the 'bridge'. On withdrawal extracellular controls were performed as usual. During some intracellular recordings the electrode potential drifted over the duration of the recording. This was probably a consequence of the electrical devices used to monitor the vital functions of the animal. We could find no remedy. Because the drift was slow it had no effect on the 4 s trial periods, and the potential could be recalibrated by monitoring the potential change when the pipette was withdrawn (Martin & Whitteridge, 1984).

The signal was continuously monitored at the preamplifier output, ADC input, and immediately after digitization to ensure the integrity of the data. The preamplifier signal was also passed through a threshold-crossing spike detector (NL200 Digitimer) whose logic output was led to the CED1401 for on-line construction of peristimulus histograms.

Visual stimuli, whose shape and trajectories were controlled on-line by microcomputer (480Z, Research Machines), were generated by a Picasso CRT Image Generator (Innisfree Ltd, USA) for display on a Hewlett Packard P1304A or Tektronix 604 oscilloscope. Their displays were synchronized with the CED1401 data logging. An AT-type microcomputer controlled the experiments by directing both the CED1401 and the 480Z. Various experimental protocols and their parameters could be selected by a menu-driven executive program that ran on the AT. In particular, any combination of stimulus size, direction, speed and contrast could be selected. The AT also maintained a comprehensive database, and provided near real-time data analysis and graphical displays that were used to monitor the progress of the experiment (Douglas & Martin, 1987).

All extracellular and intracellular recordings consisted of multiple trials. Extracellular trials were averaged to provide a peristimulus time histogram, but each intracellular trial was stored. Each trial consisted of a control period during which a neutral contrast field was displayed, followed by a test period of nearly equal duration during which the visual stimulus was displayed. For extracellular recordings the actual duration depended on stimulus parameters such as the velocity and the length of the trajectory. The intracellular trials were all of 4 s duration. The intertrial interval was at least the duration of two trials. The presentation of stimuli was randomized. For analysis of subthreshold events, action potentials were digitally stripped from the intracellular records by truncating them at their bases and then averaging the several trials.

Histology

Twelve to eighteen hours after the first neurone had been recorded, the cat was given a lethal dose of anaesthetic and then perfused through the heart with physiological saline followed by a solution of 2·5 % glutaraldehyde–1 % paraformaldehyde in phosphate buffer (pH 7·4). A Vibratome (Oxford) was used to section the tissue in the coronal plane at 80 μm. The horseradish peroxidase was revealed using the *p*-phenylenediamene–*p*-catechol method with heavy metal intensification (Perry & Linden, 1982). Shrinkage artifacts were kept to a minimum in sections containing horseradish peroxidase-filled processes by osmicating and resin embedding (Durcupan ACM, Fluka) the sections. This processing allowed the material to be examined at both the light and the electron microscopic level.

RESULTS

A total of 495 neurones was recorded from twenty-nine cats in order to obtain the results presented in these papers. Of these neurones 210 were impaled. Of these some did not respond to visual stimuli, or intracellular recordings were lost before sufficient trials could be obtained, or the quality of the intracellular data did not allow the kind of analysis being attempted here. Of the 210, forty-six neurones were suitable for analysis for this paper. They appeared representative of the entire sample in terms of their mean membrane potential and were drawn from all layers except layer 1. Of these forty-six, fifteen were identified morphologically by intracellular injection of horseradish peroxidase. Unfortunately, to obtain the long intracellular recordings necessary for this study, horseradish peroxidase injections were usually only attempted when it was clear that we were starting to lose the intracellular recording. This prevented a more complete morphological identification of the neurones recorded intracellularly. We also found that the neurones that were injected after lengthy recordings did not fill as well as neurones injected soon after impalement.

Measurements of the input resistance were made whenever possible to monitor the general condition of the particular neurone over time. We injected 50 ms square-wave current pulses and measured the voltage deflection just before the end of the pulse. This procedure required loading a different piece of software, and in some cases we lost the intracellular recording before a current–voltage plot had been made. However, in all the cases (25/46) where measurements were made, the resistance remained remarkably stable. The input resistance for neurones ranged from 10 to 153 MΩ (mean = 69 MΩ; $n = 25$). This measure of resistance did not correlate with membrane potential, or the length of the recording. It is likely that some of the variability arose because the electrode tip was located at different positions in the soma or dendrites of the neurone, with the dendrites showing higher input resistances because of their dimensions. However, high input resistances were also found in

neurones filled with HRP where the pipette track confirmed that the injection site was in the soma.

The duration of the longest intracellular recording was for 2 h 50 min, the next longest was 2 h 30 min. Although intracellular recordings in excess of 1 h were relatively rare, durations of about 0·5 h were reasonably common. However, this time window inevitably meant that many tests could not be performed on a single neurone and that in general we would have preferred to have had more trials for the averages. The data set for any single neurone varies in extent because the length of the recording time was unpredictable. In the following sections we have attempted to illustrate as wide a sample of the intracellular data as possible. Even with the forty-six neurones being considered, a considerable amount of data compression was necessary. To keep this paper below book length we have had to restrict our description and discussion of the data to a few key issues that could be concisely illustrated and described.

The results are presented in three sections, beginning with the responses of the different receptive field types to optimal stimuli, which show the subthreshold events that lead to inhibition or production of spike discharge in the receptive field. This is followed by a description of the responses to different orientations and directions of movement. As far as possible we have illustrated features of the performance of cortical neurones that were common to the different type.

Eight neurones were recorded with pipettes filled with potassium citrate and the remainder with pipettes filled with the HRP solution. All neurones could be allocated to a cortical layer on the basis of reconstructions of the electrode tracks, depth measurements, and the appearance of debris in many cases where the HRP injections were attempted but were not successful. Twelve of the neurones had complex (C-type) receptive fields; the remaining thirty-four had simple (S-type) receptive fields.

Receptive fields

Extracellular fields

During the extracellular recording the receptive fields of each eye were plotted by hand and latencies of response to electrical stimulation of the cortical afferents were determined. Bar stimuli have been the preferred stimuli for response recordings for the past 30 years, so we used them here to facilitate the interpretation of the intracellular records. The receptive fields were classified as S-type or C-type (Henry, 1977). The basis criteria for an S-type field was that its responses to moving light and dark edges were spatially segregated (see Martin & Whitteridge, 1984). These edge-induced subfields correspond to the On (light edge) or Off (dark edge) subfields that could sometimes be elicited with stationary flashed stimuli (see Berman, Douglas, Martin & Whitteridge, 1991). However, the moving edges were generally much more effective in driving the neurones than were the flashed stimuli. The features of the hand-plotted receptive fields (orientation, subfields, types) corresponded closely with those obtained by computer-controlled stimuli (Fig. 1).

Of the forty-six neurones presented here, thirty-four had S-type receptive fields and twelve had C-type receptive fields. Of the S-type fields, thirteen had a single On or Off area when mapped extracellularly (S1-type receptive fields). Nine of the thirteen (e.g. Figs 4 and 11) had intracellular profiles that resembled those of the

remaining twenty-one S-type receptive fields with more than one subfield (Figs 2, 3, 7, 9, 12 and 15). Neurones with two or more subfields would be classified as the simple cells of Hubel & Wiesel (1962). In some cases, one of which is illustrated (Fig. 4), additional subfields were revealed by intracellular recordings. The remaining four

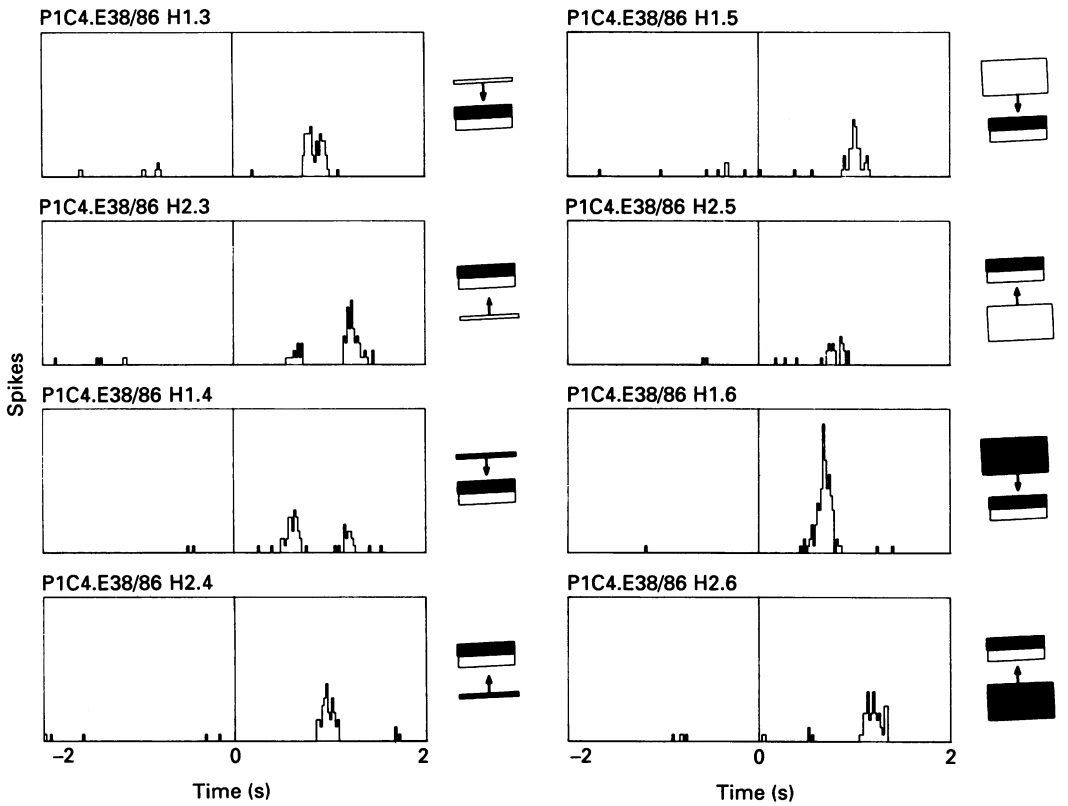

Fig. 1. Extracellular spike histograms showing the response of a layer 6 pyramidal neurone with a simple or S-type receptive field with On (light) and Off (dark) excitatory subfields. The latency to OR2 stimulation was 1·2 ms, indicative of monosynaptic activation by lateral geniculate nucleus (LGN) afferents. Each trial consists of a 2 s control period followed by a 2 s test period during which the stimulus appears and moves across the receptive field. Here each histogram represents the accumulated spikes from ten trials. The height of each window is 20 spikes, the bin width is 20 ms in this and the following figures. The schematic diagram (not to scale) shows the receptive field type and orientation preference obtained from the hand-plot. The stimulus type, contrast, orientation and direction of motion used for the digitized records is also indicated schematically. Similar conventions are used for all records. Here the left column shows responses to moving bars, the right column to moving edges. Dark-edge response corresponds to an Off response, light edge to an On response. Bar width, 0·3 deg, length 13·1 deg, velocity 3·3 deg s^{-1}. Neurone no. P1C4.E38.

neurones with S1-type receptive fields (e.g. Figs 5, 6 and 10) had intracellular profiles resembling those of the twelve neurones with C-type receptive fields (Figs 8, 13, 14, 17 and 18). However, the C-type fields responded to light and dark edges that overlapped spatially, whereas the S1-type fields, by definition, responded to a light or a dark edge, not both. The neurones with C-type receptive fields would be

classified as complex cells on the Hubel & Wiesel (1962) scheme, as would S-type neurones with a single subfield (Hubel & Wiesel, 1962; Gilbert, 1977).

In this paper we will use 'excitation' to mean an increase in action potential discharge and 'inhibition' to mean a reduction in action potential discharge,

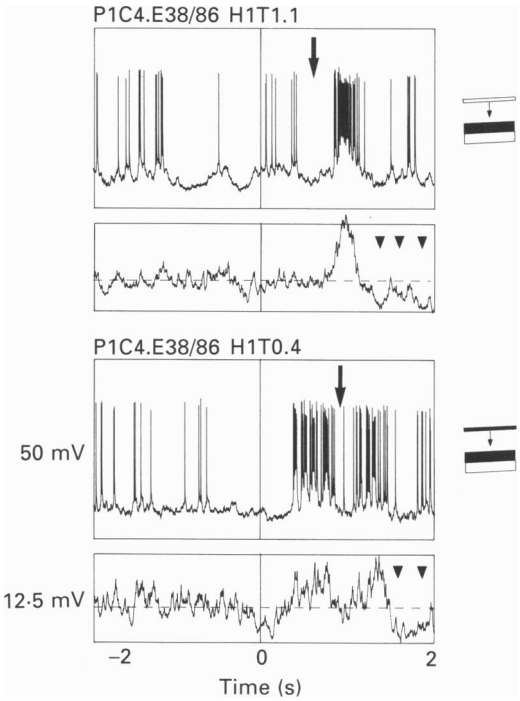

Fig. 2. Intracellular responses to moving light and dark bars for the layer 6 pyramidal neurone with a simple or S2-type receptive field, whose extracellular responses are shown in Fig. 1. Examples of the responses for single trials are shown in large windows. Each trial consists of a 2 s control period followed by a 2 s test period when the bar moves across the receptive field. Averages of several such trials including the one shown (four trials in this instance) are shown in the small windows. Action potentials have been stripped before averaging (see Methods). In this and all following figures the window height for single intracellular traces is 50 mV, and for averaged intracellular traces is 12·5 mV. The dashed line through the averaged trace indicates the mean membrane potential for the control period, in this instance −50 mV. Compare the intracellular response with the extracellular response using identical stimulus parameters shown in Fig. 1. Neurone no. P1C4.E38.

associated with the passage of the stimulus bar across the receptive field. We use this simple operational definition here, because there are a number of possible interpretations of the reduction of discharge, which we will consider in a subsequent paper (Berman *et al.* 1991).

Intracellular fields

In presenting the intracellular records, we have adopted the standard format presented in Fig. 2, which illustrates the intracellular response of a layer 6 pyramidal neurone, which was monosynaptically activated by thalamic afferents. (The extracellular responses of the same neurone are shown in Fig. 1.) All measurements

were made over a 4 s trial period, consisting of a 2 s control period, during which the spontaneous activity of the neurone was recorded, followed by a 2 s test period, during which the interleaved computer-controlled stimulus passed across the receptive field. Figure 2 (top window) shows such a trace from a single representative trial. In this and all following figures the window height for single intracellular traces is 50 mV. The membrane potential was averaged for all trials after the spikes had been stripped (see Methods), and is shown in the small window below the single trial example (Fig. 2, second window). In this and all following figures the window height for averaged intracellular traces is 12·5 mV. The dashed line through the averaged trace indicates the mean membrane potential for the control period, in this instance, −50 mV. The schematic diagram (not to scale) to the right of the traces shows the contrast, orientation, direction of motion of the stimulus and the subfield structure of the receptive field as determined from extracellular hand plots.

Such direct comparisons of extracellular and intracellular responses of the same neurone have not been made before. The important point that emerges from this comparison is that the neurones' receptive field tuning did not alter after impalement. Although some neurones became more spontaneously active and excitable after intracellular impalement, simple receptive fields remained simple, and complex fields remained complex. The directional specificity and orientation selectivity of the neurones also remained the same. In the examples presented below we have tried as far as possible to illustrate the range of intracellular behaviour observed in the different subtypes of receptive fields.

It is clear from the example (Fig. 2, top) that the membrane potential of the neurone fluctuates considerably even during the control period. Thus the concept of a 'resting' membrane potential, familiar to those working in *in vitro* preparations, is not strictly appropriate for *in vivo* recordings. For this reason it was essential that we recorded a sufficiently long control period to obtain a baseline potential against which to compare membrane potential fluctuations induced by the stimulus. The dashed line through the averaged trace indicates the mean membrane potential of the neurone during the 2 s control period for all the averaged trials.

S-type fields

The most common variety of S-type receptive field was one with two subfields (type S2; Figs 1 and 2; see Orban, 1984). This is an example of the classical 'simple cell' of Hubel & Wiesel (1959, 1962), who demonstrated that light flashed on an On subfield was excitatory, while light flashed on an Off subfield was inhibitory. On and Off subfields were found to be mutually antagonistic. A light edge moving into an On subfield excites the neurone (Fig. 1, right-hand column, top histogram), as does a dark edge moving into an Off area (Fig. 1, right-hand column, third from top histogram). The bar responses are more complex than the edge responses (Fig. 1, left-hand column), because bars have two edges, one leading and one trailing.

The light bar moving through the receptive field (Fig. 2, top) elicited a strong discharge as the bar left the Off subfield (the Off excitatory response) and entered the On subfield (the On excitatory response). This shows the synergy of On and Off excitatory responses in simple receptive fields, originally reported by Hubel & Wiesel (1959, 1962). As the light bar left the On subfield (i.e. the On subfield went dark) and

moved into the region flanking the receptive field, spontaneous discharge was inhibited. This was associated with a hyperpolarization of the membrane (arrow-heads in averaged trace).

With the dark bar, a complementary pattern of activation was obtained. As the dark bar moved into the Off subfield, the membrane potential depolarized to

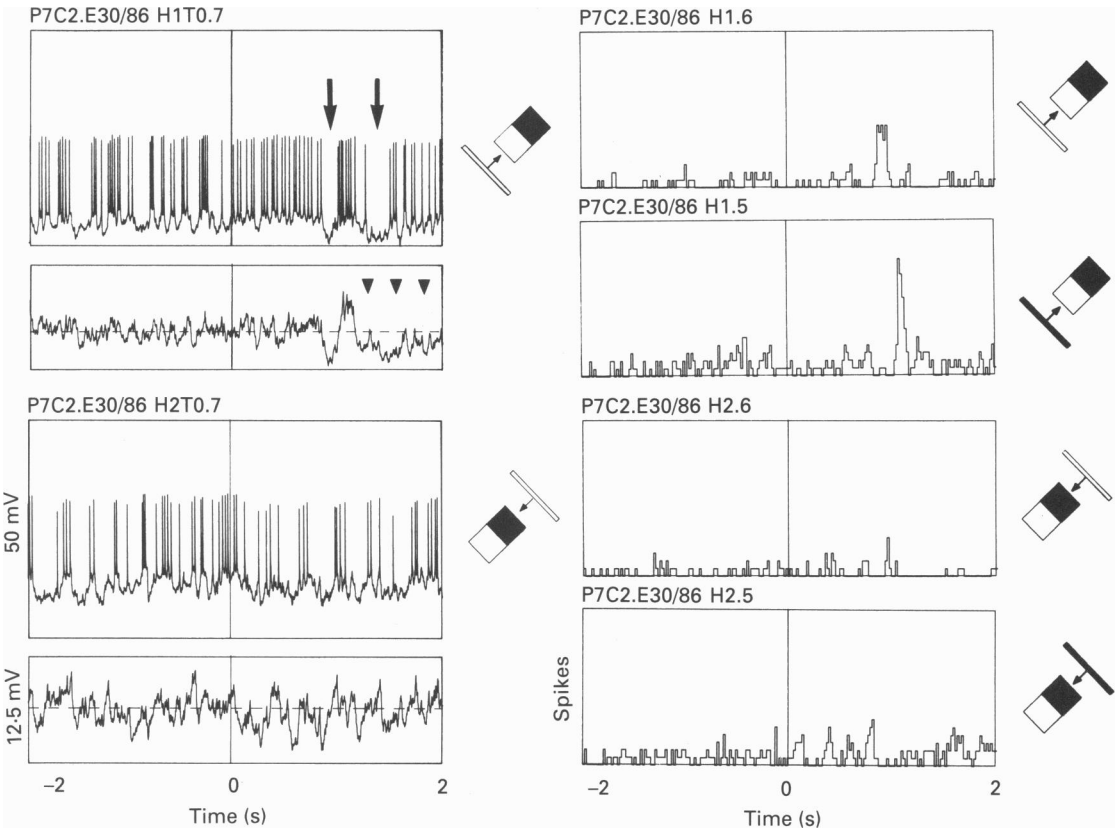

Fig. 3. S2-type receptive field of a neurone recorded in layer 4, morphology unknown. Left column shows intracellular recordings, right column shows extracellular spike histogram obtained before the neurone was penetrated (window height 40 spikes). The directionality was contrast independent. The neurone showed spontaneous activity in extracellular recordings, which increased due to depolarization after impalement. This discharge was completely inhibited (arrows in single intracellular trace) as the light bar moved through receptive subfields in the optimal direction. The hyperpolarization associated with this inhibition is evident in the averaged trace, but extends (arrow-heads in averaged trace, five trials; mean potential = −30 mV) beyond the zone of complete inhibition. This strong inhibition is absent with bar movement in the non-optimal direction in either the extracellular or intracellular records. Bar width 0·3 deg, length 5·3 deg, velocity 3·3 deg s^{-1}. Neurone no. P7C2.E30.

threshold and initiated a train of action potentials. As the dark bar entered the On subfield there was an inhibition of the discharge (arrowed), followed by a strong discharge as the dark bar left the On subfield. Spontaneous activity was then inhibited as the bar moved into the region flanking the receptive field. This was

associated with hyperpolarization of the membrane (arrow-heads in averaged trace). Note that the intracellular excitatory responses from this neurone were spatially equivalent to the extracellular discharge. The main point of difference between the extracellular and intracellular records was that in the latter the spontaneous activity is slightly higher and the responses were stronger.

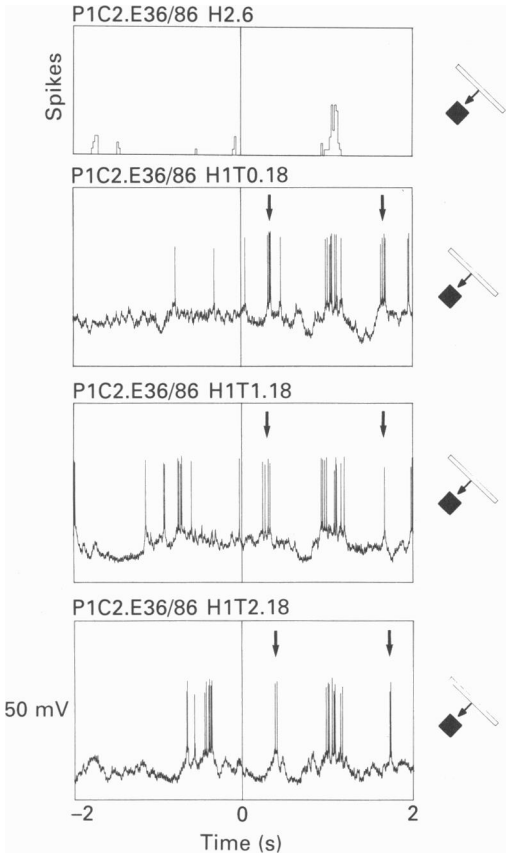

Fig. 4. S1-type Off receptive field of a neurone recorded in layer 3, morphology unknown. The latency of response to OR2 stimulation was 2·8 ms, indicative of polysynaptic (indirect) activation by LGN afferents. The hand-plot and extracellular spike histogram (top trace, fifteen trials, window height 40 spikes) showed a single Off region. However, the intracellular penetration increased excitability and revealed additional subfields that gave rise to depolarizations leading to action potentials (arrowed in all three trials), separated by hyperpolarizations and associated inhibition. An average of the membrane potential is also shown in Fig. 11 (mean potential −43 mV). Bar width 0·3 deg, length 6·0 deg, velocity 3·0 deg s^{-1}. Neurone no. P1C2.E36.

The subfield antagonism elicited by moving bars was seen most clearly in spontaneously active neurones, as shown in Fig. 3. This neurone, recorded in layer 4, was discharging spontaneously before impalement, as the extracellular histograms show (right-hand columns). The spontaneous activity increased when the neurone was depolarized by the impalement, but the spontaneous activity was completely inhibited (arrows) as the bar moved across the subfields. This inhibition was

associated with distinct membrane hyperpolarizations (see averaged trace). The presence of the first hyperpolarization (see averaged trace) was unexpected because the hand-plotted field and the extracellular recording with the dark bar (right-hand column, second from top) did not reveal a second Off subfield. Unfortunately, the

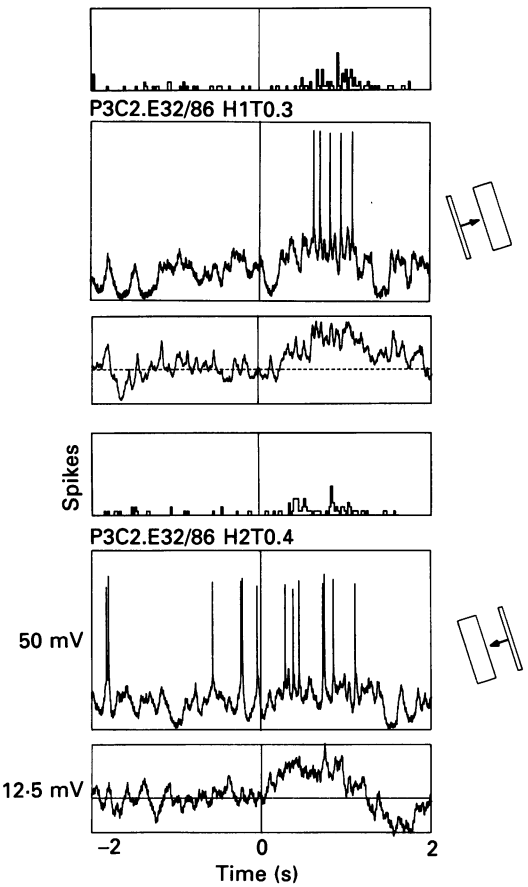

Fig. 5. S1-type On receptive field of a layer 2 neurone recorded with a potassium citrate-filled pipette. The latency of response to OR1 stimulation was 4·7 ms, indicative of polysynaptic activation by LGN afferents. Extracellular spike histograms (three trials; window height 20 spikes) show single On region. The slow, monomodal depolarization evident in the averaged trace (six trials; mean potential −64 mV) is in marked contrast to the peaks and troughs of the membrane potential evident in Figs 3 and 4. Bar width 0·3 deg, length 13·1 deg, velocity 3·3 deg s^{-1}. Neurone no. P3C2.E32.

intracellular recording was lost before we could stimulate the neurone with a dark bar. In the reverse direction of motion, the extracellular histograms (Fig. 3, right-hand column) revealed little or no excitation or inhibition evident with bars of either polarity. This form of directionality will be considered further in the section 'Direction Selectivity' below.

All eighteen S2-type receptive fields showed some spatial separation of inhibition and excitation in response to a moving bar. However, the pattern of action potential

discharge was not a reliable predictor of the changes in membrane potential. This was most apparent in the S1-type receptive fields, which responded to either a dark or light edge. Nine of the thirteen neurones with S1-type receptive fields had intracellular records that closely resembled those found in neurones with S2-type receptive fields.

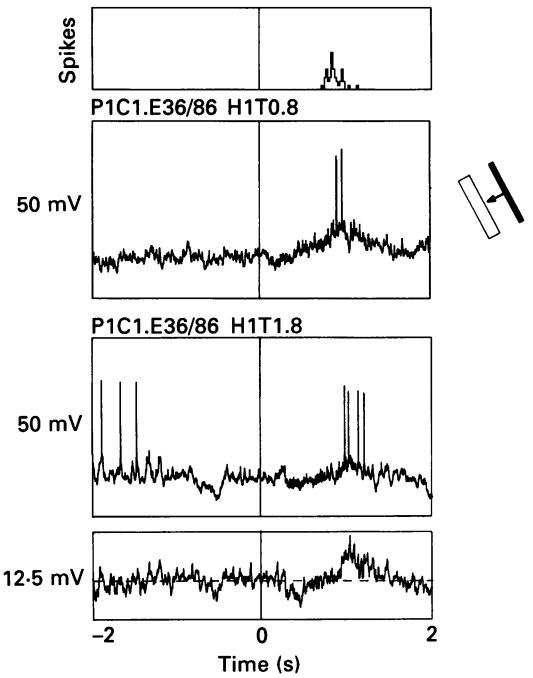

Fig. 6. S1-type On field showing response to dark bar. The neurone was recorded in layer 3, morphology unknown. The latency of response to OR1 was 3·3 ms and to OR2 was 2·7 ms, indicative of polysynaptic input from LGN afferents. Extracellular spike histogram (three trials; window height 20 spikes) shows discharge as dark bar leaves On region. Two examples of single trials, and an averaged trace (three trials; mean potential −53 mV), show a slow rise to action potential threshold, as in Fig. 5, and a lack of the discrete hyperpolarizing subfields seen in some S1-type receptive fields (e.g. Fig. 4). Bar width 0·3 deg, length 12·0 deg, velocity 3·0 deg s^{-1}. Neurone no. P1C1.E36.

Intracellular recording from one neurone with an S1-type field (Fig. 4) revealed additional subfields. This neurone, recorded in layer 3, responded to a single dark edge, and to both a dark (not shown) and a light bar (Fig. 4).

This neurone responded with a gradual depolarization of the potential until the action potential threshold was reached. This profile contrasts with the rapid and spatially discrete transitions seen in the majority of neurones with S-type fields (e.g. Figs 2, 3 and 4). In this respect such S-type fields resembled those of the C-type receptive fields (described below).

Although neurones with S1-type receptive fields only responded to an edge of one contrast, they did respond to bars of the opposite contrast, as shown in Fig. 6 (compare with Fig. 4). This neurone, recorded in layer 3, responded to a light edge, but could be driven by a dark bar. Presumably the neurone is responding to the

trailing edge of the light bar. Here the slow depolarization leading to action potential discharge suggests that the excitatory inputs to these neurones are weaker and more spatially dispersed than those of the archetypical simple receptive fields.

The remaining three neurones with S-type receptive fields had three subfields. The layer 5 pyramidal neurone shown in Fig. 7 responded strongly to moving bars and

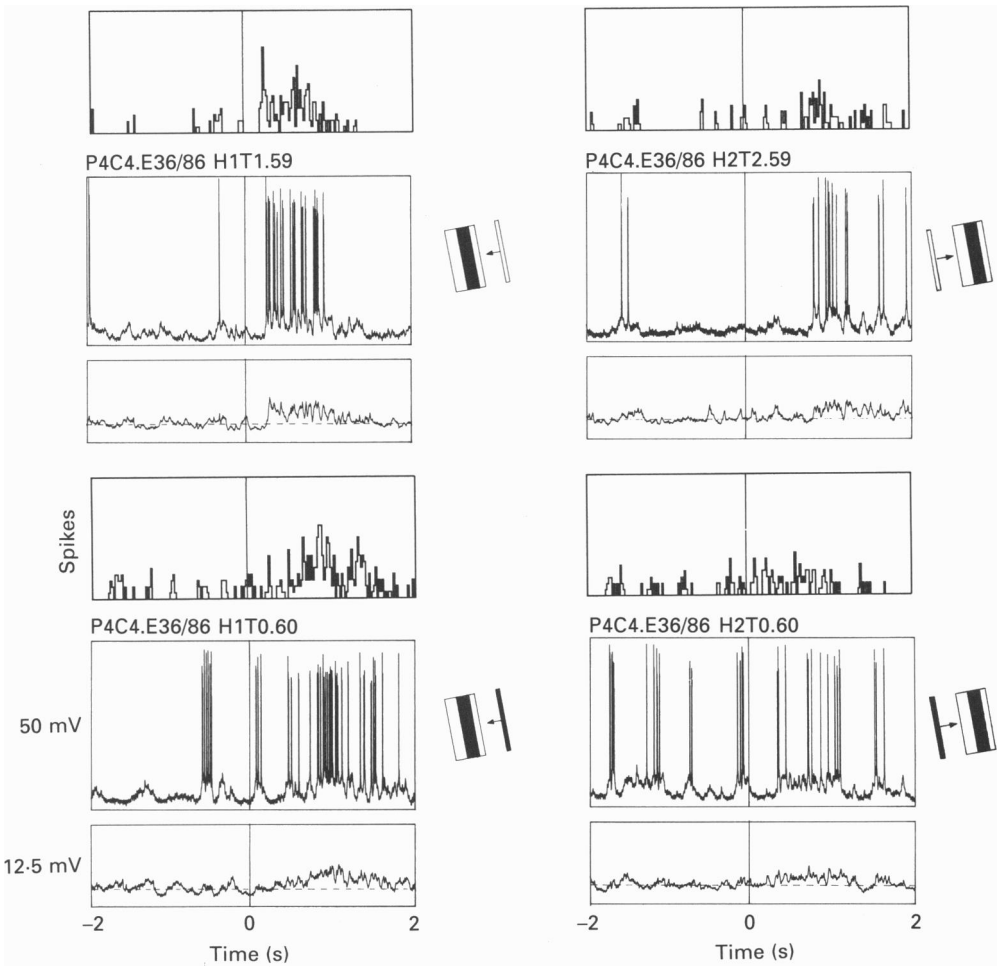

Fig. 7. S3-type receptive field of a pyramidal neurone recorded in layer 5. The latency of response to OR1 stimulation was 3·0 ms and 2·2 ms for OR2, indicating polysynaptic activation from LGN afferents. The averaged potentials (three trials; mean potential −60 mV) show spatial separation in their peaks, but no indication of discrete subfield hyperpolarization seen in other S-type receptive fields (e.g. Figs 3 and 4). Note that the optimal direction of motion is the same for light or dark bars. Extracellular spike histograms, three trials; window height 20 spikes. Bar width 0·3 deg, length 12·0 deg, velocity 3·0 deg s^{-1}. Neurone no. P4C4.E36.

edges, and the dark bar and light bar responses were spatially separate, as in S2-type receptive fields (Fig. 2). However, the response of this neurone resembled that of C-type receptive fields in having no distinct hyperpolarizations between the subfields.

C-type fields

All the C-type receptive fields are equivalent to the complex receptive fields of Hubel & Wiesel (1962). Following Gilbert's (1977) classification of the complex receptive fields into 'special' (showing little length summation) and 'standard'

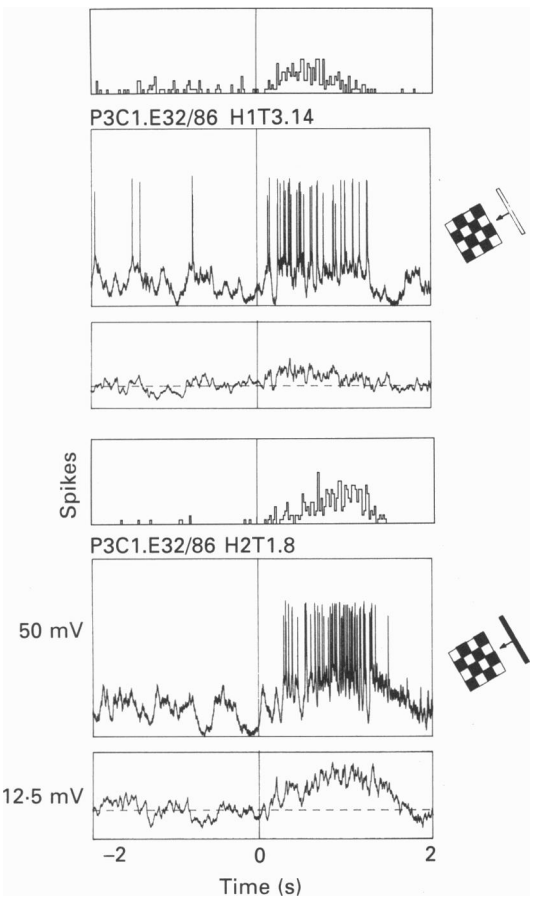

Fig. 8. Complex or C-type receptive field (indicated by chequered schematic) of a neurone recorded in layer 3. The latency of response to stimulation at OR2 was 2·8 ms, indicating polysynaptic activation by LGN afferents. The receptive field shows different sensitivities to light and dark bars, although the discharge regions overlap (compare with S-type fields, e.g. Figs 2 and 7). Extracellular spike histograms (four trials; window height 20 spikes), single trial, and averaged (four trials; mean potential −60 mV) membrane potential show that C-type receptive fields have larger width than S-type fields. Bar width 0·7 deg, length 13·1 deg, velocity 3·3 deg s^{-1}. Neurone no. P3C1.E32.

(showing considerable length summation), we have called these receptive field types C_{SP} and C_{ST} respectively. Eight of the twelve C-type receptive fields showed strong length summation and were classified as C_{ST}. In all cases the stimuli used were long bars, so that the summation profiles were not examined intracellularly. Intracellular recordings could not otherwise distinguish between the two groups.

The sustained action potential discharge of neurones with C-type receptive fields was generated by an extensive underlying depolarizing potential (Fig. 8). The single plateau of depolarization seen in this layer 3 neurone contrasts with the alternating hills and valleys of excitation and inhibition seen within most S-type receptive fields.

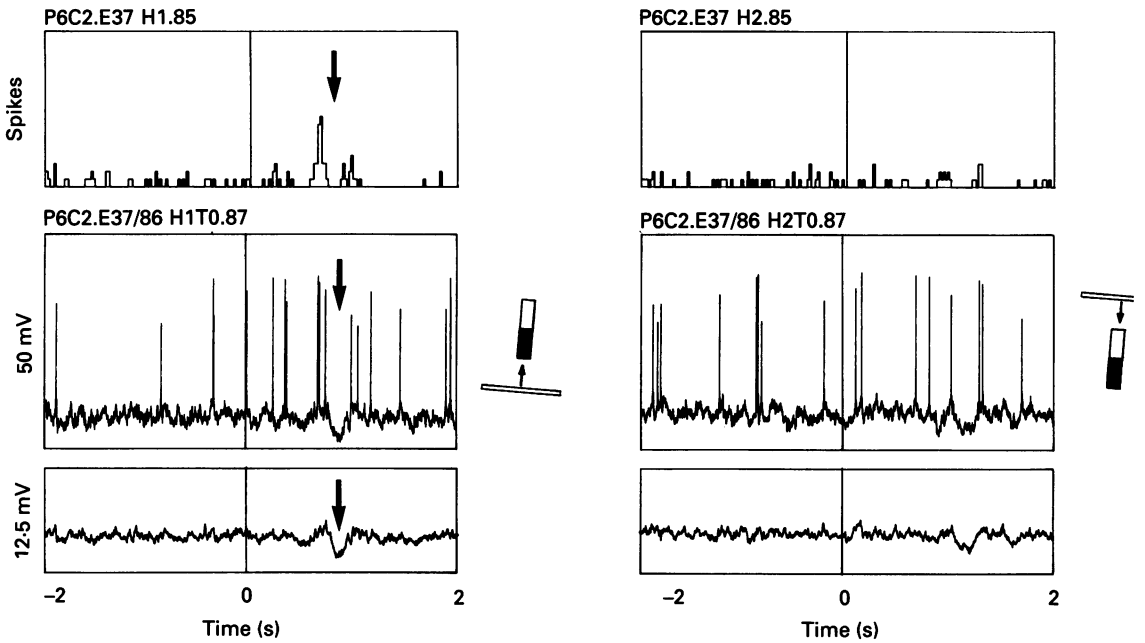

Fig. 9. S2-type receptive field recorded from a spiny stellate neurone in layer 4. The latency of response to OR2 stimulation was 1·2 ms, indicating monosynaptic activation from LGN afferents. The extracellular histograms (three trials; window height 40 spikes) show that the neurone is strongly directional, as would be predicted from the subfield arrangement. The intracellular recording shows a very localized burst of activity in the optimal direction of motion (left-hand traces), which is followed by a region of inhibition (arrowed). In the non-preferred direction of motion (right-hand traces) there was no excitatory response. Averaged traces, three trials; mean potential −33 mV for both directions of motion. Bar width 0·3 deg, length 11·3 deg, velocity 2·8 deg s^{-1}. Neurone no. P6C2.E37

The overlapping On and Off responses that define the C-type receptive fields meant that both light and dark bars elicited a similar response pattern. This contrasts markedly with the S-type receptive fields where the response to the light and dark bars could differ markedly, both in spatial position and sensitivity. Within the C-type receptive field, however, the response was rarely a smoothly sustained discharge. As originally noted by Hubel & Wiesel (1962), bursts of action potentials were interrupted by repolarizations from the plateau of the depolarization. This is clearly seen in the single trials in Fig. 8.

The response to light bars, although overlapping with that of the dark bars, could differ in sensitivity through the receptive field. In the example shown, the response to the dark bar is stronger than the light bar response and appears stronger in one portion of the field. (This feature has also been noted using stationary flashed stimuli as in the line-weighting functions by Movshon *et al.* 1978*a*, *b*.) In five of twelve C-type receptive fields the region of spike discharge was followed by a period in which

spontaneous activity was consistently absent. In this inhibitory zone the membrane was sometimes hyperpolarized relative to the mean baseline potential, but could also just return to the baseline potential, as previously described by Creutzfeldt *et al.* (1974).

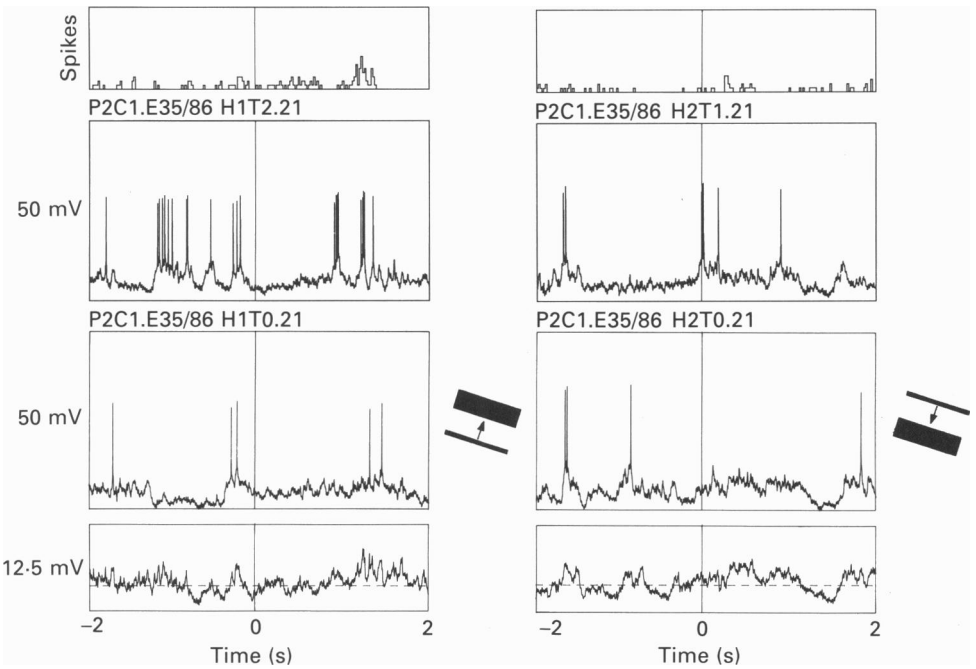

Fig. 10. S1-type Off receptive field of a layer 6 pyramidal neurone. A slow depolarization leads to action potentials in the optimal direction of motion (left-hand traces). In the non-optimal direction (right-hand traces) there is no clear excitatory response (averaged traces: left, three trials; right, five trials; mean potential −50 mV). Extracellular spike histograms, three trials; window height 20 spikes. Bar width 0·5 deg, length 10·6 deg, velocity 2·7 deg s^{-1}. Neurone no. P2C1.E35.

Direction selectivity

The majority of neurones we recorded from showed some degree of direction preference to a moving stimulus. The cumulative evidence from extracellular studies is that directionality is generated by intracortical inhibitory processes (Hubel & Wiesel, 1962; Goodwin, Henry & Bishop, 1975; Sillito, 1977; Duysens & Orban, 1981; Emerson & Coleman, 1981; Palmer & Davis, 1981*a*, *b*; Ganz & Felder, 1984). The dominant model for directionality is that originally proposed for the rabbit retina by Barlow & Levick (1965) but later adapted for cortex by Barlow (1981) and others (Dean, Hess & Tolhurst, 1980; Ganz & Felder, 1984; Emerson, Citron, Felleman & Kaas, 1985; Koch & Poggio, 1985). In the Barlow–Levick model, directionality depends on the phase relationship of postsynaptic inhibition and excitation. When the stimulus is moved in the non-preferred direction, inhibition and excitation occur coincidently, producing a net reduction or elimination of the excitatory response. In the preferred direction the stimulus evokes the same magnitude of inhibition, but the inhibition is delayed with respect to the excitation,

so the neurone discharges. Thus, their model makes the simple prediction that intracellular recordings should show that strong inhibition follows the excitatory response in the preferred direction. Here we consider only the case of directionality using bar stimuli moving orthogonally to the optimal orientation.

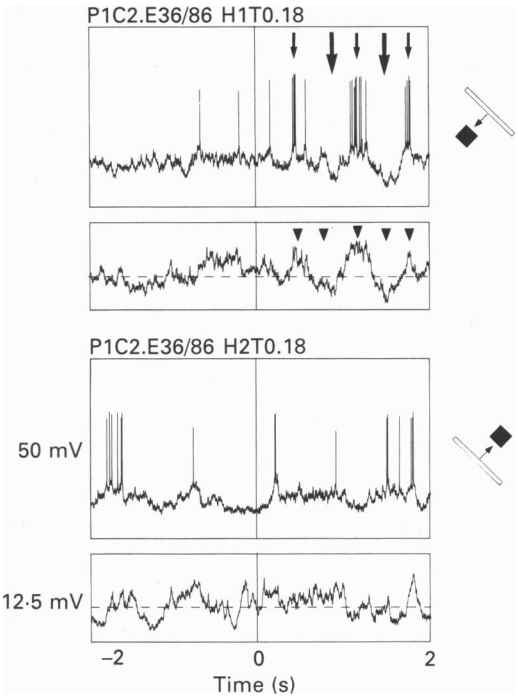

Fig. 11. S1-type Off receptive field (same cell as in Fig. 4). Movement in the optimal direction (upper traces) elicits a strong discharge (small arrows) interrupted by two hyperpolarizations (large arrows). Arrow-heads in averaged traces (three trials; mean potential −53 mV), indicate peaks and troughs in membrane potential response. No response is seen in the non-optimal direction (lower traces). Neurone no. P1C2.E36.

S-type receptive fields

The subfields of S-type or simple receptive fields offer a means of constructing the Barlow–Levick circuit for direction selectivity. On and Off subfields of simple receptive fields are mutually inhibitory and thus a spatial asymmetry in the arrangement of subfields should produce a directional preference (Hubel & Wiesel, 1962). This basic phenomenon is illustrated in Fig. 9 for a spiny stellate neurone of layer 4, which had an S2-type receptive field and was monosynaptically activated by X-like thalamic afferents. The extracellular histograms (top traces) show that the neurone was completely directional. The strongest discharge occurred at the transition between the subfields, as the light bar moved out of the Off subfield into the On subfield. The inhibition following the excitatory discharge was clearly seen as the bar moved out of the On subfield (arrows; inhibition of action potential discharge in extracellular histogram; hyperpolarizing potential, middle and lower traces). In the non-optimal direction, the excitation due to the light bar moving into the On subfield was counteracted by the antagonistic inhibition produced by the bar moving

out of the On subfield and into the Off subfield. This is the pattern predicted by the Barlow–Levick model and first observed in simple cells by Hubel & Wiesel (1959, 1962).

The hypothesis that the phase relations of excitation and inhibition determine the direction preference of neurones with S-type receptive fields receives additional

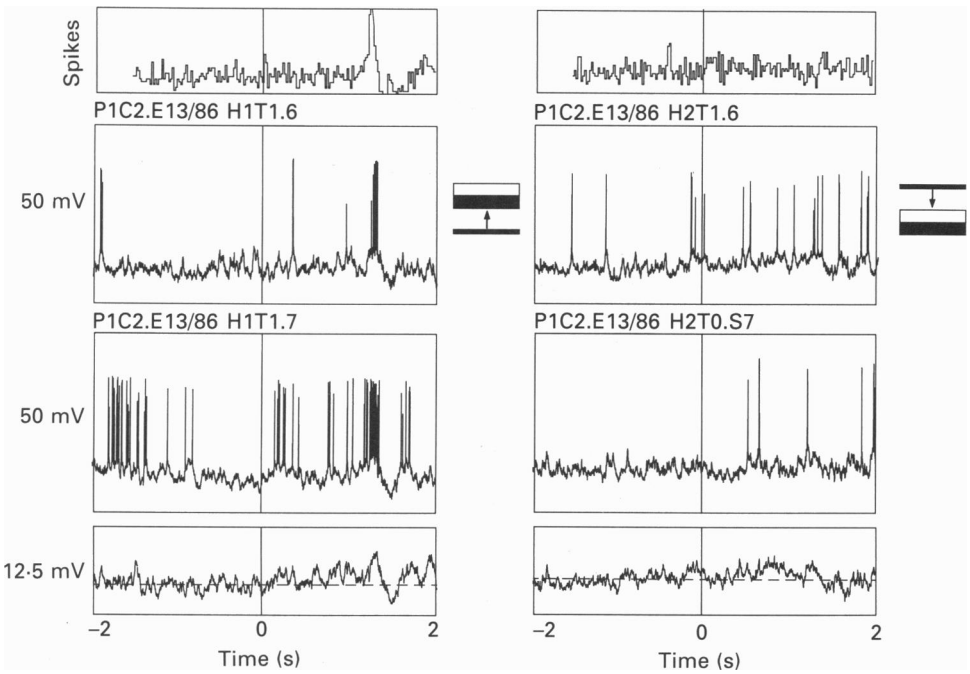

Fig. 12. S2-type receptive field of a layer 4 neurone, morphology unknown. Latency to stimulation from optic chiasm was 3·4 ms, from OR1 1·3 ms, and from OR2 0·8 ms. These indicate that the neurone was monosynaptically activated by X-like LGN afferents. The strong biphasic response in the single trial (top trace), and the averaged membrane potential (four trials, second trace) in the optimal direction, contrasts with the lack of response in the non-optimal direction (bottom traces). Extracellular spike histograms, five trials; window height, 30 spikes. Bar width 0·3 deg, length 10·0 deg, velocity 2·5 deg s^{-1}. Neurone no. P1C2.E13.

support from the rare cases of non-directional S-type receptive fields. An example of one of these is shown in Fig. 5. This field is one of the four examples of S1-type fields that did not have the characteristic inhibitory subfields of all other S-type fields. In this example the dark bar moving across the receptive field gave an approximately equivalent response in both directions. A bar of opposite polarity also gave a non-directional response. Although this example is consistent with the Barlow–Levick model, there are many simple cells whose directional preferences are not obviously explained by their model. Five different examples are presented below.

The first example is from a layer 6 pyramidal neurone, which has an S1-type receptive field with no hyperpolarizing subfields (Fig. 10). In this example a dark bar was moved across the single Off subfield. In the preferred direction (left-hand traces) there was a slow depolarization leading to an action potential discharge, followed by

a slow return to the baseline. The discharge was rather weak and inconsistent from trial to trial. But, when the same bar was moved in the reverse direction (right-hand traces) there was no action potential discharge. Its location in layer 6 makes it likely that this neurone received direct excitation from the non-directional neurones in the

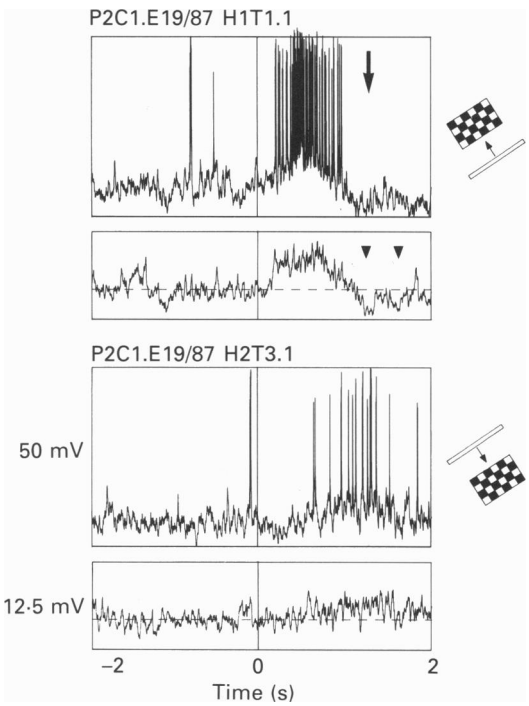

Fig. 13. C-type receptive field of a layer 3 pyramidal neurone. Latency to stimulation at OR1 of 3·2 ms indicates that the neurone was polysynaptically activated by LGN afferents. An antidromic response was evoked from OR2 with a latency of 1·2 ms. The strong discharge in the optimal direction of motion (top traces) is followed by a hyperpolarization (arrowed), clearly visible in the averaged trace (arrow-heads, three trials; mean potential −60 mV). Bar width 0·3 deg, length 10·2 deg, velocity 2·5 deg s^{-1}. Neurone no. P2C1.E19/87.

lateral geniculate nucleus (Bullier & Henry, 1979; Ferster & Lindström, 1983; Martin & Whitteridge, 1984). If this were so, the inhibitory input to the neurone would have to be directionally tuned to explain our observation.

In cases where the S1-type fields had inhibitory zones lying to either side of the excitatory centre, there were no obvious asymmetries that would suggest directional selectivity. In the event, some of these neurones were strongly directional as shown in Fig. 11 (see also Fig. 4). Extracellular recordings (not illustrated) from this layer 3 neurone showed that its directional response was contrast dependent. The intracellular recording showed a very symmetrical arrangement of excitation and inhibition as the bar moved in the optimal direction. In the reverse direction none of these fluctuations were evident. On the basis of the Barlow–Levick model, it is not obvious how this very symmetrical arrangement of subfields would lead to the strong directional selectivity exhibited by this neurone.

Directional preferences counter to that predicted from the subfield arrangements

were also observed in neurones with S2-type fields. Figure 3 shows a neurone that is directionally selective regardless of the polarity of the bar (Fig. 3 extracellular histograms, right-hand column). The intracellular records from this neurone reveal a central zone of excitatory discharge flanked by inhibitory subfields (small arrow,

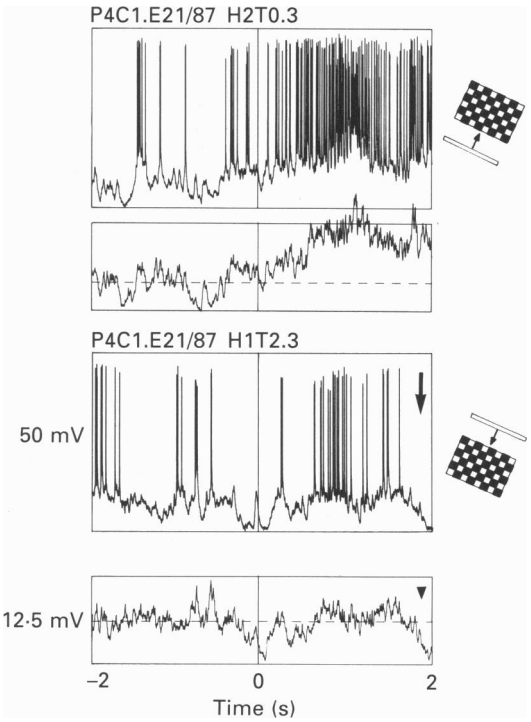

Fig. 14. C_{ST}-type receptive field of a layer 3 pyramidal neurone. Latency to stimulation from OX was 4·8 ms, from OR1, 3·0 ms and from OR2, 1·9 ms. These values are intermediate and could indicate mono- or polysynaptic drive from either X or Y LGN afferents. In the optimal direction the bar does not pass out of the very large receptive field (average, four trials). In the non-optimal direction the bar begins moving within the receptive field but does not initially elicit a depolarizing response. A clear hyperpolarization (arrow-head in average, three trials; mean potential −65 mV) is elicited as the bar leaves the field. Bar width 0·2 deg, length 10·2 deg, velocity 2·5 deg s^{-1}. Neurone no. P4C1.E21/87.

arrow-heads in average). Despite this apparent symmetry in subfield organization, this neurone was strongly direction selective. The neurone was located in layer 4 and almost certainly received direct input from non-directional neurones of the lateral geniculate nucleus (Bullier & Henry, 1979; Ferster & Lindström, 1983; Martin & Whitteridge, 1984). Despite this there is no evidence of an excitatory input during stimulation in the non-optimal direction.

Anomalous direction preferences were also found in S-type receptive fields that did have clear asymmetries in the receptive field organization. In the S2-type receptive field shown in Fig. 12, the subfield antagonism predicts that the optimal response should occur when the bar leaves an On subfield and enters an Off subfield (Hubel & Wiesel, 1962), but in fact the optimal response was in the reverse direction. A strong

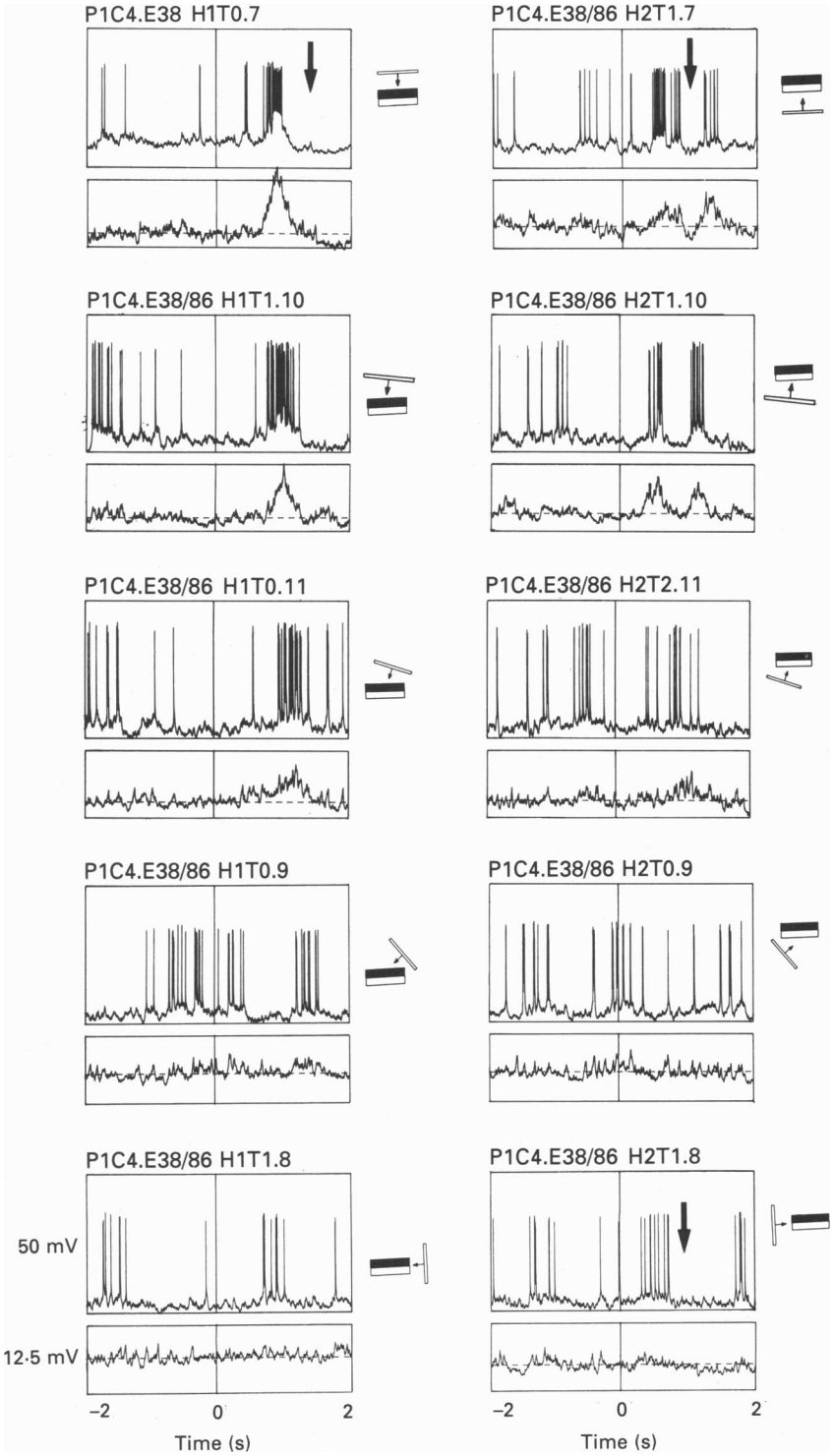

Fig. 15. For legend see facing page.

discharge (top trace, large arrow) was evoked when the dark bar moved first through the Off and then through the On subfield. A subsidiary excitatory subfield (small arrow) was not seen in the extracellular recording (not shown). In the reverse direction (lower traces) the neurone did not respond and the marked membrane fluctuations seen in the averaged trace for the preferred direction of motion were absent. This neurone was not tested quantitatively with a light bar so it is not known whether the directionality was polarity independent.

The neurone shown in Fig. 12 was located in layer 4 and received monosynaptic (direct) excitation from afferents of the lateral geniculate nucleus. The centre-surround receptive fields of the geniculate neurones are non-directional. Hence the clear lack of excitation in the non-optimal direction would seem to require postsynaptic inhibition. Yet there was no evidence from the intracellular records of hyperpolarizing potentials, which are normally associated with postsynaptic inhibition. (See also Fig. 16, right-hand column, for a monosynaptically activated directional neurone of layer 4, where inhibition of action potential discharge is clearly in evidence in the non-preferred direction of motion.)

The final example is of a layer 5 pyramidal neurone with an S3-type receptive field. In this example (Fig. 7), the directionality was independent of the polarity of the stimulus. Stimulation of the neurone at the optimal direction of motion (left-hand column) with either light or dark bars did not reveal any hyperpolarizing inhibitory subfields (see averaged traces, left-hand column) that might give rise to a directional response. Yet stimulation with either light or dark bars in the non-preferred direction (right-hand column) showed that the response was considerably reduced. The averaged traces revealed no indication of a hyperpolarization in membrane potential. In other S3-type receptive fields, however, the inhibition associated with directionality was sufficient to inhibit completely the spontaneous activity as shown in Fig. 16 (middle traces, left-hand column, arrowed).

C-type receptive fields

Nine of the twelve neurones with C-type receptive fields had no strong directional preferences. This differs from the S-type fields, where the vast majority were strongly directional (see Orban, 1984). A directional C-type receptive field is shown in Fig. 13, where the bar moving in the optimal direction (upper traces) reveals an inhibitory (hyperpolarized) subfield that follows the strong excitatory discharge (arrowed in top trace, arrow-heads in averaged trace). In the reverse direction (lower traces) this inhibitory subfield is not in evidence and the excitatory discharge is considerably reduced. This is the form of response predicted by the Barlow–Levick model.

However, the following example suggests that an inhibitory subfield located at one side of the excitatory zone may not be a sufficient explanation of the mechanisms of directionality in C-type receptive fields. In the example shown in Fig. 14 the

Fig. 15. S2-type receptive field of a layer 6 pyramidal neurone (same neurone as Figs 1 and 2) showing response to different orientations of a moving bar. Discrete hyperpolarizing potentials are only visible around the optimal orientations (single arrows in top traces). Inhibition of spontaneous activity (arrow, bottom right trace) was seen at the cross orientation. Averages are of five trials; mean potential −50 mV. Bar width 0·3 deg, length 13·1 deg, velocity 3·3 deg s^{-1}.

receptive field was so large that in the optimal direction (upper traces) the edge of the field extended beyond the excursion of the bar. The strong response of the neurone (note the irregular discharge, upper trace) continued until the last point was collected in the sweep. This meant that in the reverse direction the bar actually began to move within the excitatory receptive field. Thus, an inhibitory flank lying outside the excitatory field, such as that illustrated in Fig. 13, could not be activated. Nevertheless, the response in the reverse direction was very much weaker than that in the optimal direction. Thus, if the directionality was being generated by inhibitory processes, they would have to be activated from within the receptive field itself.

Orientation selectivity

All the neurones studied in this paper were orientation selective, as assessed using moving stimuli. The selectivity revealed in this way corresponds closely to the selectivity obtained with stationary flashed stimuli. There is good evidence (reviewed in Martin, 1988) that intracortical inhibitory mechanisms are involved in orientation selectivity, but the exact role of inhibition remains unclear. In the following section we describe the membrane events underlying orientation selectivity.

S-type receptive fields

Ten of the thirty-four neurones with S-type receptive fields were tested with non-optimal orientations during intracellular recording. An example of the orientation selectivity of one of these neurones is given in Fig. 15. In this example the strongest hyperpolarization was seen at the optimal orientation (arrowed, top left and right traces). As the stimulus was moved away from the optimal (upper to lower traces, left- and right-hand sides), the amplitude of polarizations rapidly decreased. At the cross-orientation, i.e. 90 deg to the optimal orientation, the spontaneous activity was inhibited (e.g. bottom right-hand trace, arrow), but there was little sign of membrane hyperpolarization.

As in the example shown in Fig. 15, the membrane polarization in response to the cross-oriented stimulus was insignificant for most neurones with S-type fields. This is consistent with the results from our extracellular recordings from spontaneously active neurones (Fig. 16). For both neurones, the strongest inhibition of spontaneous discharge was found at the optimal orientation with the optimal direction of motion (Fig. 16, top traces). In the reverse direction (middle traces) strong inhibition was also seen (arrowed), which presumably contributes to the very directional response. At the cross-orientation (lower traces) significant inhibition is present for the neurone shown in the left-hand trace (arrowed), but not for the second example (right-hand traces).

C-type receptive fields

Eight of the twelve C-type neurones were tested with non-optimal orientations during intracellular recording. An example of one of these neurones tested over a range of different orientations is shown in Fig. 17. This series maps out the orientation tuning in 10 deg intervals. Evident in all the records was the broad plateau of depolarization that is characteristic of the complex or C-type receptive fields. Depolarizations were present even when no action potentials were elicited by the passage of the stimulus. A hyperpolarization that follows the action potential

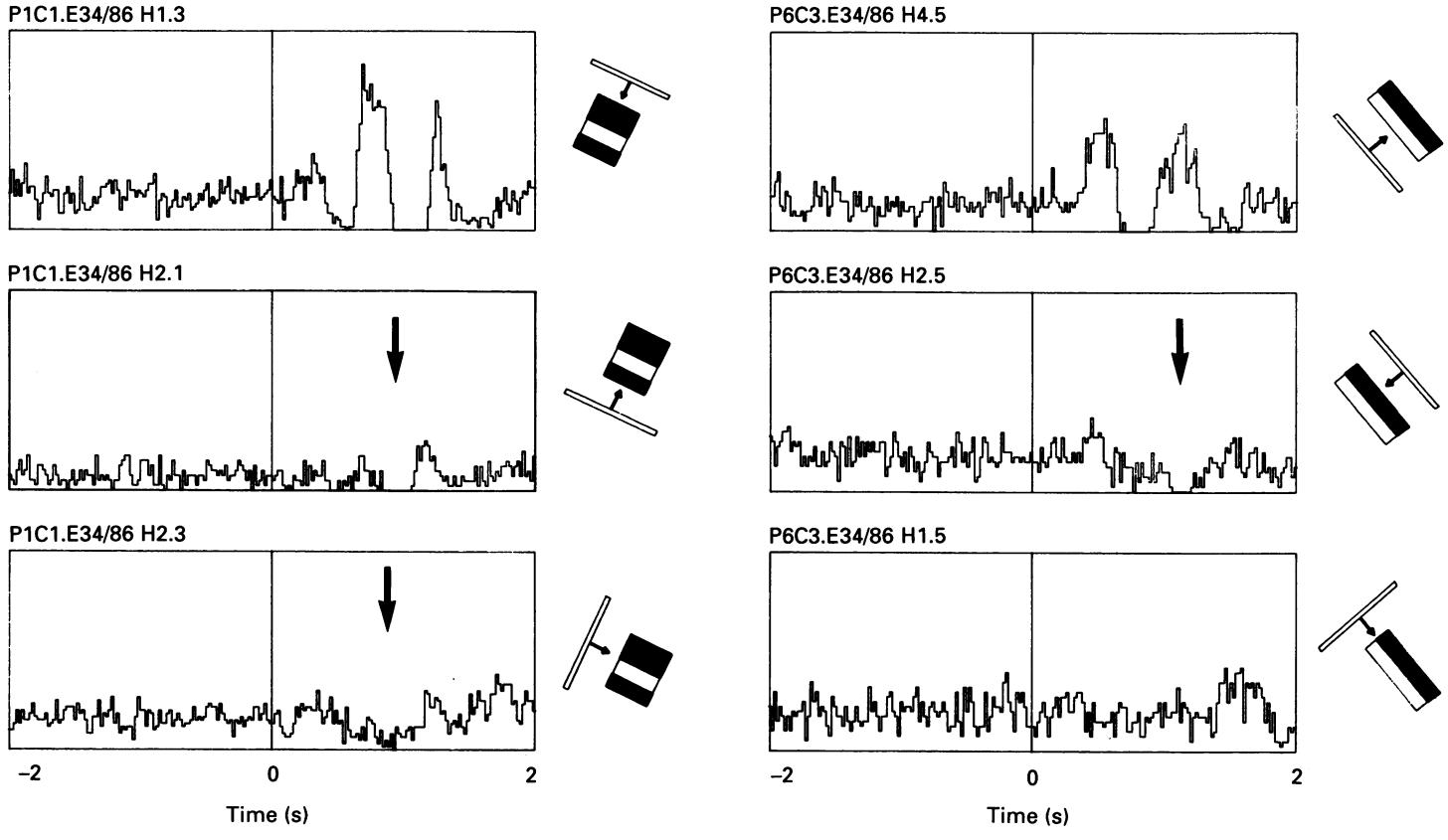

Fig. 16. Extracellular responses recorded from two spontaneously active neurones with directionally selective S-type receptive fields. In both cases (top histograms: left, twenty-one trials; right, twenty-three trials) the optimal orientation and direction of motion produces strong excitation and inhibition. In the non-optimal direction (middle histograms: left, fifteen trials; right, twenty-three trials) there is no excitatory response and the spontaneous activity is completely inhibited for a brief period (arrowed). At the 90 deg cross-orientation (lower histograms: left, twenty-one trials; right, twenty-three trials) the spontaneous activity is significantly inhibited (> 2 S.D.s from control mean) for the neurone shown on the left (arrowed), but not for the neurone shown on the right. The recordings in the left-hand column were made from a neurone in layer 5 or 6, morphology unknown, latency to OR1 stimulation 2·2 ms, to OR2 2·0 ms, indicating polysynaptic activation by LGN afferents. Bar width 0·6 deg, length 11·6 deg, velocity 2·9 deg s^{-1}. The neurone in the right-hand column was recorded in layer 4, morphology unknown, latency of response to OX stimulation 4·0 ms, to OR1 stimulation 2·0 ms, probably monosynaptically activated by X-like LGN afferents. Bar width 0·3 deg, length 11·6 deg, velocity 2·9 deg s^{-1}. Neither neurone was successfully impaled for intracellular recording. Window height: left, 60 spikes; right, 40 spikes.

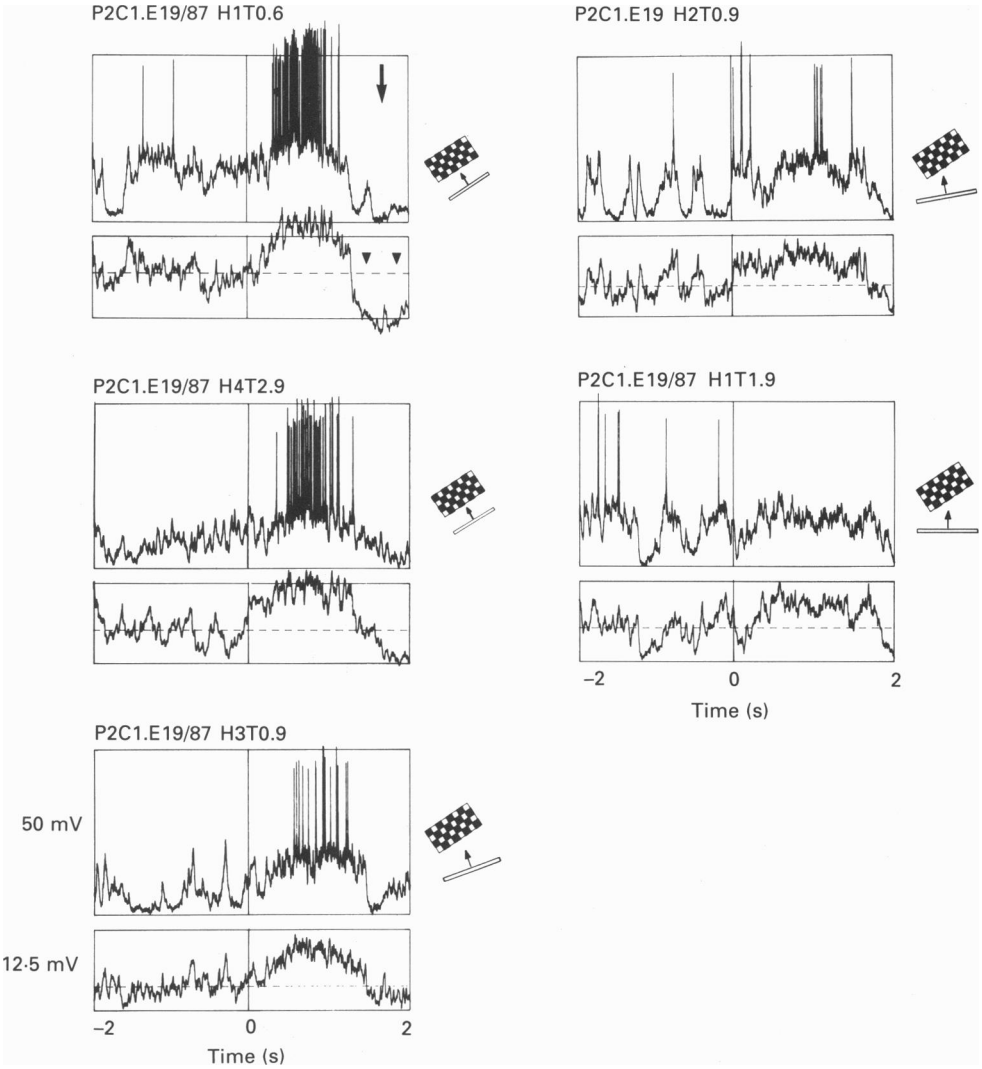

Fig. 17. For legend see facing page.

discharge was also evident in many of the traces (e.g. arrow and arrow-heads, top left traces). At the cross-orientation (90 deg off optimal) the stimulus evoked a depolarization that did not reach threshold (bottom right-hand traces). This is in distinct contrast to the intracellular observations made for S-type receptive fields (Fig. 15).

Figure 18 shows another C-type receptive field tested over the full range of orientations in 30 deg steps. As with the previous example there was a plateau of depolarization. For orientations near optimal, the plateau of depolarization extended almost the full width of the bar excursion. However, in contrast to the example shown in Fig. 17, a hyperpolarization and associated inhibition of the action potential discharge was revealed when the bar was only 30 deg off the optimal orientation and remained in evidence to the extremes of the tuning curve. The

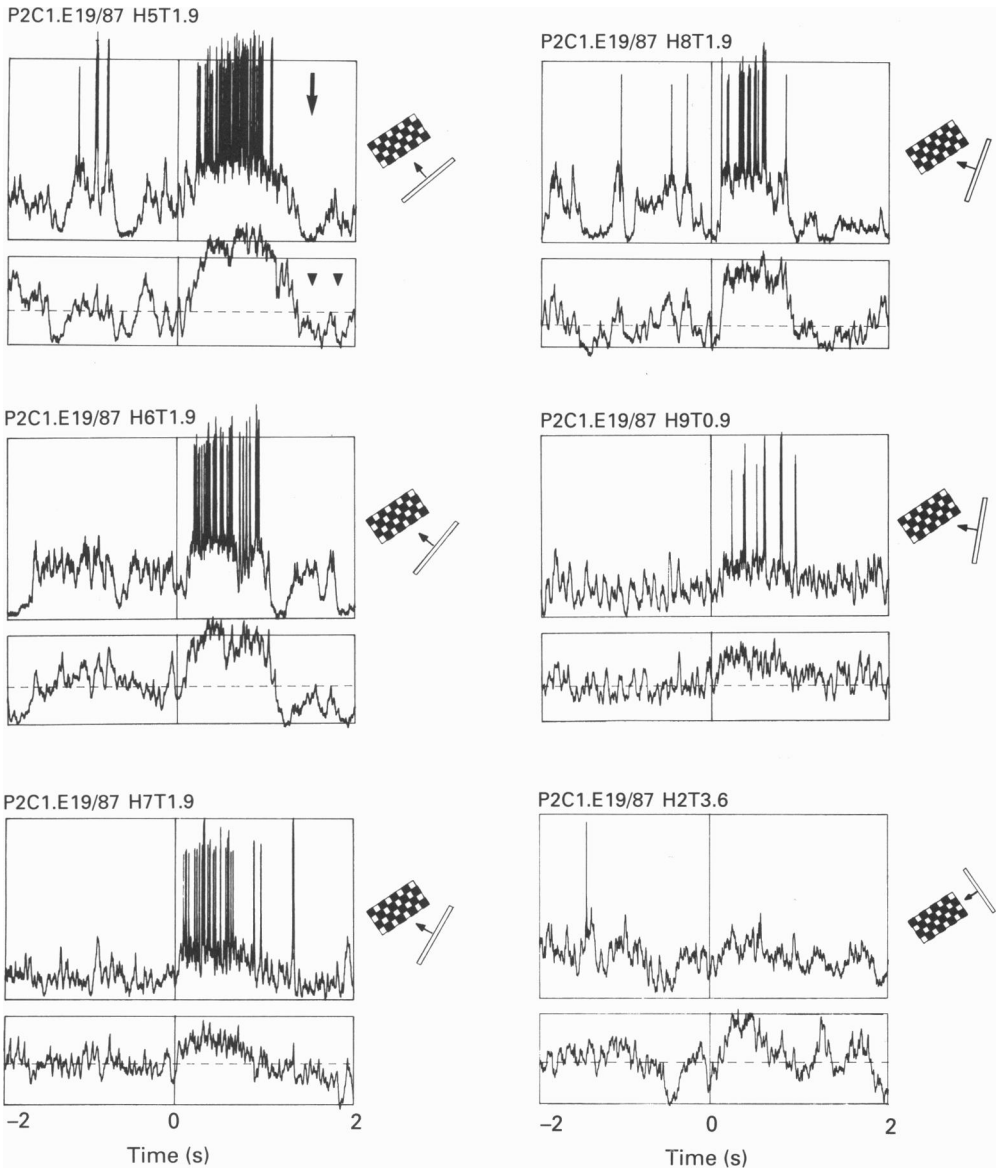

Fig. 17. C-type receptive field of a layer 3 pyramidal neurone (same neurone as Fig. 14). Orientation tuning shown in 10 deg steps, clockwise rotation for left-hand page, anticlockwise for right-hand page. Hyperpolarization follows periods of strong stimulus-driven discharge (e.g. top left-hand trace, arrowed in single trace, arrow-heads in average, three trials; mean potential −60 mV), but depolarization is seen at the 90 deg cross-orientation (right-hand bottom trace average). Bar width 0·3 deg, length 10·2 deg, velocity 2·5 deg s^{-1}.

orientation-sensitive inhibition was extensive in this case. Although the hyperpolarization could inhibit a spontaneous discharge (e.g. bottom right-hand trace), spontaneous action potentials did break through these hyperpolarizing periods, suggesting that the inhibition was relatively weak.

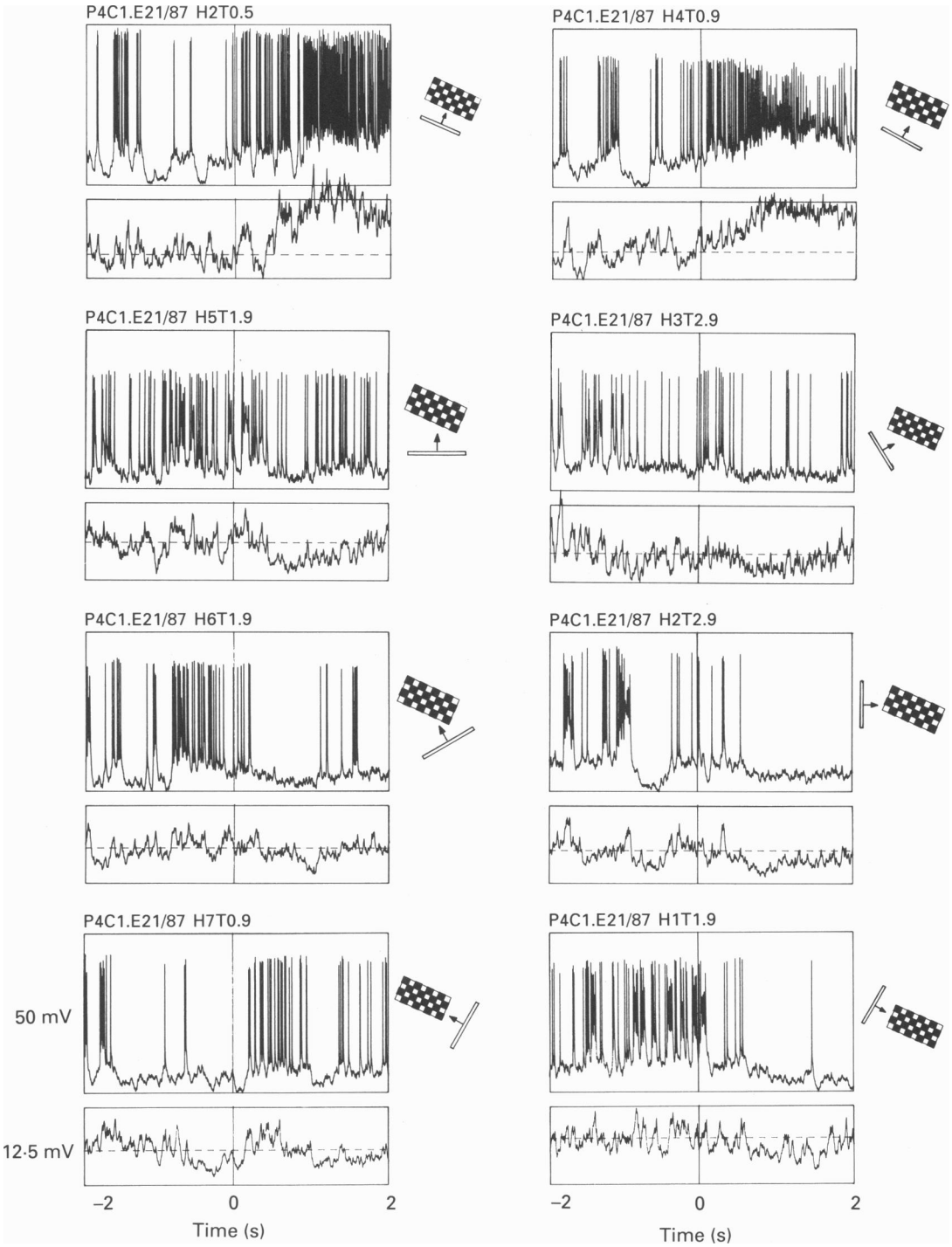

Fig. 18. C_{ST}-type receptive field of layer 3 pyramidal neurone (same neurone as Fig. 14). Tuning curve in 30 deg steps shows inhibition of action potential discharge (single traces) associated with hyperpolarization (averaged traces, three trials) as the stimulus moves off optimal orientation. Bar width 0·2 deg, length 10·2 deg, velocity 2·5 deg s^{-1}.

DISCUSSION

Although a great many issues arise out of this series of experiments, for the sake of brevity we will concentrate here on aspects of the physiology that illuminate the organization of the local circuitry and its function. We hope that this analysis will lead to a better understanding of the interaction of excitation and inhibition that produces the characteristic receptive field structure and selective responses of neurones in cat visual cortex.

For the purposes of this paper we have operationally defined inhibition as a reduction in action potential discharge induced by the stimulus. This definition necessarily includes the possibility that inhibition is occurring at an earlier stage in the circuit, so we are detecting a withdrawal of excitation. It also includes the possibility that the inhibition following an excitatory discharge is due to the intrinsic membrane currents that underlie the post-train after-hyperpolarization seen in neurones in cortical slices (Schwindt, Spain, Foehring, Chubb & Crill, 1988). However, there are at least two conditions where the involvement of postsynaptic inhibition has been demonstrated repeatedly and unequivocally. The first is that of subfield antagonism in simple cells and the second is in directionality.

The evidence for postsynaptic inhibition in subfield antagonism and directionality will be discussed below. The degree to which inhibition is involved in orientation selectivity, however, remains a contentious issue. The two extremes are represented by Sillito (1984); 'the inhibitory system is seen to be the architect of orientation selectivity' and Ferster (1987); 'orientation of receptive fields is neither created nor sharpened by inhibition between neurones with different orientation preference.'

The structure of receptive fields

In most neurones we were able to map the receptive field extracellularly, using hand-plotting and computer-controlled stimuli before recording the intracellular responses to the same moving stimuli. The two broad classes of response that could be distinguished from the averaged membrane potentials correspond closely to the simple and complex classification of Hubel & Wiesel (1962) or the S- and C-type scheme of Henry (1977), which we have used. As Orban (1984; p. 113) has reviewed and discussed in detail, the main point of difference between these two schemes lies in the classification of receptive fields that had a single On or Off field (the S1-type field here). Some authors have called these fields complex and others have called them simple or S-type (see p. 113 of Orban, 1984 for a critical review). All C-type receptive fields would be classified as complex, and all S-type fields with more than one subfield (two of three in our sample) would be classified as simple. Our intracellular recordings show that most S1-type receptive fields closely resemble those of simple cells. A minority of neurones (4/13) with S1-type receptive fields had intracellular responses that are more like those of complex, or C-type, receptive fields. But for the majority, the terms C or complex, and S or simple, can be used interchangeably, on the basis of the membrane potential patterns.

A defining feature of simple receptive fields is that there is antagonism between the subfields (Hubel & Wiesel, 1962). In their earliest study Hubel & Wiesel (1959) showed that this antagonism was due to intracortical inhibition. Subsequent analyses of simple receptive fields by the Canberra group who used stationary and

moving stimuli (Bishop *et al.* 1971; Bishop, Coombs & Henry, 1973) and by others (e.g. Movshon *et al.* 1978*a*, *b*; Palmer & Davis, 1981*a*; Heggelund, 1981*a*; see Orban, 1984 for review) confirmed the original observations of Hubel & Wiesel (1959, 1962) that there is mutual inhibition between the subfields of simple or S-type receptive fields.

The antagonism between the subfields cannot be accounted for simply by a subcortical mechanism; Heggelund (1981*a*) reported that the centre-surround antagonism of geniculate neurones was too weak to account for the strong antagonistic inhibition (70–100% of control) he detected between the subfields of simple cells. The simplest explanation is that the cortical inhibitory neurones are involved. The inhibition is probably mediated by GABAergic synapses since the structure of the subfields can be disrupted by *n*-*m*-bicuculline application (Sillito, 1975). It is this subfield inhibition that is responsible, at least in part, for the complex membrane potential fluctuations we observed in twenty of the twenty-four S-type receptive fields reported here.

In the case of both simple and complex cells, the action potential discharge, even for the optimal stimulus, gives an incomplete reflection of the underlying changes in membrane potential. For simple cells it is particularly difficult to predict the potential changes from the spike output. For example, a polyphasic perturbation in membrane potential may underlie a monophasic burst of action potentials as the stimulus moves through the receptive fields. In extracellular recordings there is also no measure of the depth of the hyperpolarization, which we found to vary in simple receptive fields. In complex cells the membrane potential generally showed a more monophasic response, although hyperpolarizations often followed the excitatory discharge. In the intracellular responses of complex cells we found a monophasic depolarization, regardless of the polarity and direction of movement of the stimulus. In simple cells, by contrast, a number of separate depolarizations were interleaved with periods of hyperpolarization and/or inhibition of the spike discharge. If receptive fields were classified on the basis of their membrane potential then the monophasic response of complex cells is more 'simple' than the polyphasic response of simple cells.

Both S- and C-type receptive fields had a fringe of subthreshold synaptic activity, inhibitory, or excitatory, or both, that preceded or followed region(s) of spike discharge. For some neurones, this fringe was several times broader than the zone from which spike discharge was recorded. The vast majority of neurones with S-type receptive fields had clear subfields where the response to a moving bar was inhibited. Many neurones of both S- and C-type receptive fields had an inhibitory zone following the main discharge. Because this inhibition was independent of the contrast of the stimulus, it may be due to the intrinsic membrane conductances responsible for the post-train hyperpolarization seen in *in vitro* experiments (Connors, Gutnick & Prince, 1982). However, the temporal duration of synaptic inhibition could also account for the hyperpolarizations (see Douglas & Martin, 1990).

In a previous intracellular study (Ferster, 1988) evidence was presented that the inhibitory fields in simple and complex cells were co-extensive with excitatory fields. In a number of instances we did not find this co-extensivity. Instead zones were found where the action potential discharge was inhibited with both light and dark

bars or where inhibition with a stimulus of one polarity was not associated with a complementary excitation by a stimulus of the opposite polarity, as has been suggested previously from extracellular recordings (Emerson & Gerstein, 1977*a*). Thus, the inhibitory and excitatory inputs to these neurones are functionally not completely co-extensive. For simple cells, the polarity-independent inhibition could well be provided by complex cells. Complex cell inhibition of simple cells has previously been suggested to explain the failure of simple receptive fields to respond to textured patterns that excite complex cells (Hammond & MacKay, 1977; Burr, Morrone & Maffei, 1981).

Hubel & Wiesel suggested that the convergent input of many simple cells of the same orientation selectivity would be sufficient to build a complex receptive field (Hubel & Wiesel, 1962). However, this model did not make explicit why the properties of directionality and stimulus contrast sensitivity that are so characteristic of simple cells are not features of complex cells. In general, if the dominant input of the complex cells is to be from other simple cells then the simple cells will have to be from a large pool with sufficient variety in contrast sensitivity, direction selectivity and spatial position to produce the common non-directional complex cell. The polyphasic membrane perturbations so characteristic of the input to most simple cells is removed from their output (essentially through half-wave rectification, suggested by Movshon *et al.* 1978*a*, *b*). Convergent input of this rectified signal to complex cells could account for the essentially monophasic profile of membrane depolarization that is characteristic of complex cells.

The notion of high convergence fits well with our anatomical and theoretical investigations (Martin & Whitteridge, 1984; Douglas, Martin & Whitteridge, 1987; reviewed in Martin, 1984, 1988), which show that there is a high divergence in the output from a single neurone and suggest that one neurone supplies only a small component of the excitatory input to any other neurone. Large unitary excitatory postsynaptic potentials (EPSPs) are not apparent in our intracellular records and this agrees with experimental work using cross-correlation techniques, which shows that the functional connection between one cell and another is weak (Toyama, Kimura & Tanaka, 1981; T'so, Gilbert & Wiesel, 1986). Such a weak linkage between single neurones contains the further implication that lateral geniculate afferents and other complex cells could also contribute in a major way to the pattern of inputs to complex cells observed here.

For simple receptive fields the possible circuitry is more restricted because of a number of factors, including the dependence of the excitatory response on the stimulus contrast, the constraints on the spatial localization and polarity (On or Off) of the subfields, and the direction selectivity. Within these constraints, both lateral geniculate afferents and other simple cells could provide the excitatory input to simple cells. However, complex cells could only contribute an excitatory input to simple cells under the restricted condition that the complex excitation be a relatively small component of the total excitation arriving at the simple cell. This is necessary because the discharge of complex cells is independent of the stimulus contrast, whereas the subfields of simple cells gives excitation with one contrast and inhibition with the opposite contrast.

A further layer of complexity is added by the differences in the pattern of action

potential discharge in response to visual stimulation. Hubel & Wiesel (1962, 1965) observed that complex cells tend to have a much more bursty pattern of discharge than simple cells. Similar patterns were evident in our intracellular records. The trains of action potentials elicited from complex receptive fields were punctuated with zones of partial repolarization. Although the various patterns of discharge may be determined by different patterns of activation, differences in membrane properties may also influence the pattern.

The classic complex receptive fields are found in the deep cortical layers, particularly layer 5. It is in these same layers that the 'bursting' cells have been found in preparations of cortical slices (Connors *et al.* 1982). These neurones respond to a depolarizing current step with a high-frequency burst of three to five spikes followed by a large hyperpolarization (Berman, Bush & Douglas, 1989). A similar mechanism may be present in the deep-layer complex cells *in vivo*. The current injected into a neurone by a visually activated synapse is unlikely to be in the form of a steady step, so that this mechanism may be continually reactivated as the stimulus moves through the receptive field.

Direction selectivity

Most simple cells in our sample were directional when tested with stimuli of the optimal orientation. Although in some cases directionality can be explained in terms of the organization of the On and Off subfields, as has been reported previously (Hubel & Wiesel, 1962; Palmer & Davis, 1981*b*), there are many instances where the direction preference is the same for light and dark bars (Emerson & Gerstein, 1977*a*, *b*; Albus, 1980) and thus cannot be accounted for by receptive field asymmetries. Previous studies explain contrast-independent directionality on the basis of inhibitory regions (Goodwin *et al.* 1975; Emerson & Gerstein, 1977*b*; Duysens & Orban, 1981; Emerson & Coleman, 1981; Palmer & Davis, 1981*b*; Ganz & Felder, 1984; Eysel, Muche & Wörgötter, 1988). However, extracellular recordings have suggested that disinhibitory, or facilitatory, mechanisms may also operate, perhaps in tandem with inhibition (Emerson & Gerstein, 1977*b*; Movshon *et al.* 1978*b*; Ganz & Felder, 1984). Consequently, two different mechanisms need to be considered, one inhibitory, one facilitatory.

Directional mechanisms involving inhibition usually adopt a version of the model suggested by Barlow & Levick (1965) to account for the direction selectivity of ganglion cells in the rabbit retina. In their model, two detectors are connected to an And–Not gate (a non-linear logical device that gives an output only when its first input is on and its second input is off). If the two inputs arrive simultaneously at the gate, there is no output. In the cortex, the And–Not gate would be realized by postsynaptic interaction of excitatory and inhibitory inputs, perhaps on the head of a spine (Koch & Poggio, 1985). The conjunction of an excitatory and inhibitory input to a neurone (the gate) would lead to no response, but the arrival of the inhibitory input before or after the excitatory input would allow the excitation through. The alternative mechanism of facilitation could follow the same arrangement of detectors and delay lines as above, but replace the And–Not gate with a device that multiplies excitatory inputs. The non-linearity inherent in the multiplication would eliminate the need for inhibition. Directionality could then be produced by simply amplifying

the excitation in the preferred direction. The delay here could be introduced through a multisynaptic cortical pathway.

The intracellular recordings can provide an indication as to the mechanisms that might be operating. We know that the neurones of the A-layers of the lateral geniculate nucleus are not directionally selective. Simple cells that get a monosynaptic excitation from lateral geniculate afferents should therefore exhibit non-directional excitation if no other processes intervene. In fact, a feature of most simple cells, including those in layer 4 (our Figs 9, 12 and 16) is that they have a directional preference (see Orban, 1984). If a multiplicative excitatory mechanism is acting then in response to motion in the non-preferred direction we would expect an excitatory depolarization, due to the direct geniculate drive, but no amplification of this response by the delayed input from intracortical sources. In the preferred direction the intracortical multiplier is engaged, which would then amplify a relatively small excitation arriving from the geniculate nucleus.

However, the directional simple cells did not give an excitatory depolarizing potential for the non-preferred direction of motion. Instead the response of the membrane potential in the non-preferred direction was virtually flat, or even hyperpolarized, despite the unavoidable conclusion that the geniculocortical synapses on the neurone were active. Thus, we have to suppose that for the non-preferred direction, inhibitory processes are acting postsynaptically to reduce the excitation that arises from the geniculate afferents. Thus the directionality of simple cells cannot be accounted for by an entirely multiplicative mechanism of feedforward facilitation. This conclusion is consistent with data from extracellular recordings in which the GABA receptors have been antagonized with bicuculline (Sillito, 1975, 1977; Tsumoto, Eckart & Creutzfeldt, 1979). Almost all simple cells and many complex cells lost their direction selectivity when bicuculline was applied ionophoretically in the vicinity of the neurone.

Extracellular recordings reveal inhibition by the suppression of spontaneous activity as the stimulus moves in the non-preferred direction (Figs 12 and 16). In some of the intracellular recordings shown here the membrane hyperpolarized as the stimulus moved in the non-preferred direction, as had previously been reported by Innocenti & Fiore (1974). However, it should be noted that these polarizations were never large, usually about 5 mV maximum. The magnitude of outward current needed to produce this change in the membrane potential is in fact quite small (for E_{rev} approximately -80 mV), perhaps fractions of a nanoampere for the neurones recorded here. This suggests that the inhibitory currents may be calibrated so as to reduce, or cut off, the action potential discharge without driving the membrane potential to such negative values that the neurone becomes insensitive to additional excitation.

The mechanism of directionality in complex cells has not been studied as extensively as that in simple cells. Pharmacological studies in which bicuculline was ionophoretically applied to complex cells has produced variable results: some neurones lose directional selectivity, others seem resistant (Sillito, 1977). Differences between S- and C-type receptive fields were also noted in experiments designed to remove lateral inhibition by inactivating local regions of the cortex using GABA (Eysel *et al.* 1988). Disinhibition was found more frequently for cells with S-type

receptive fields. Using other experimental protocols, Goodwin *et al.* (1975) found no inhibition of spontaneous activity in complex cells when the stimulus was moved in the non-preferred direction. This suggests that complex cells receive their excitation from directionally tuned neurones. Different results from the same establishment were obtained by Bishop, Kato & Orban (1980) who found that spontaneous activity could be inhibited in complex cells that were completely direction selective.

We did not record from any neurones with complex or C-type receptive fields that were completely direction selective: only four of twelve neurones showed strong directional preferences and all the neurones responded to the non-preferred direction of motion. The simplest explanation of directionality is that the excitatory input is directional. Alternatively, an inhibitory input may be activated in the non-optimal direction, but is insufficiently strong to suppress totally the excitatory input. What appears then is the sum of the inhibitory and excitatory inputs. Although we found evidence for a contrast-independent inhibition following the excitatory discharge in the preferred direction of motion, such regions are unlikely to be able to sustain the directionality throughout the relatively large receptive fields of complex cells. In the following paper (Berman *et al.* 1991) we examine whether shunting mechanisms underlie direction selectivity in complex cells.

Orientation selectivity

Orientation selectivity is thought to be generated by one of two possible ways. In one type of model, for example that suggested by Hubel & Wiesel (1962) for both complex and simple cells, the orientation selectivity is provided by excitatory processes alone. The selectivity arises through a precise selection of the units that are to provide the convergent excitation. In the second type of model, for example those of Bishop *et al.* (1973) and Heggelund (1981*a*, *b*) inhibitory mechanisms were introduced to inhibit the response to the non-optimal orientations.

In most studies the inhibition associated with orientation selectivity has been investigated using extracellular recording (e.g. Bishop *et al.* 1973; Sillito, 1975, 1979; Nelson & Frost, 1978; Ramoa *et al.* 1986; Bonds, 1989). In a few instances intracellular recording has also been used, but there is substantial disagreement on the data. Creutzfeldt *et al.* (1974) provided support from intracellular recording for the view that inhibition was involved in orientation tuning. However, they found that the strongest inhibition was elicited with stimuli close to the optimal orientation. A very different picture was painted by Ferster (1986) who, on the basis of his intracellular data, concluded that inhibition was not involved in orientation selectivity at all.

The results from the present series of experiments indicate that there was a wide variation in the response of different neurones when tested with non-optimal orientations. In agreement with others (Benevento, Creutzfeldt & Kuhnt, 1972; Creutzfeldt *et al.* 1974; Ferster, 1986, 1987, 1988), we found that neurones with S-type or simple receptive fields showed little change in the resting membrane potential in response to stimulation at the non-optimal orientation inhibition. The most marked depolarizations and hyperpolarizations were evoked with the optimal stimulus. This was also seen in extracellular recordings from spontaneously active simple cells, where in some cases there was no inhibition of the spontaneous activity for non-optimal orientations (Ferster, 1981; Fig. 16 of present study).

Even for neurones receiving monosynaptic activation from the lateral geniculate afferents, the intracellular records showed that in most cases the membrane potential was unperturbed by the passage of the cross-oriented stimulus. This picture is strongly reminiscent of what we found for the directionally selective simple cells discussed above. At the cross-orientation at least some of the geniculate inputs to monosynaptically driven neurones should be active, yet none of this activity was visible postsynaptically. We suggested for directional selectivity that inhibition might be responsible for eliminating a subthreshold depolarization. A similar suggestion applies here.

Ferster (1987, 1988) attempted to make the synaptic currents more visible by injecting caesium ions into neurones to raise their input resistance and thereby make synaptic potentials more visible. Unfortunately, he did not report the response of the neurone prior to caesium ion injections, so his observation that the neurones depolarized in response to cross-orientation stimulation is difficult to interpret. Ferster concluded that there is no cross-orientation inhibition, but since caesium ions are known to block potassium channels, it seems possible that the caesium injections alter the balance in favour of excitatory synapses by blocking outward potassium currents that might otherwise have an inhibitory effect.

Neurones with complex or C-type receptive fields had strong depolarizations over a range of non-optimal orientations, a phenomenon that no doubt underlies the broad orientation tuning that is characteristic of complex cells in the cat. In some of the complex cells we found strong inhibition just off optimal orientations, as seen previously in extracellular recordings in visual cortex (DeValois, Yund & Hepler, 1982). In others, the depolarizations were found for all orientations, although action potentials were not evoked at extreme non-optimal orientations. In such neurones, an excitatory response to an optimally oriented stimulus may in fact be facilitated by simultaneous cross-orientation stimulation.

The very broad orientation tuning of inhibitory potentials in complex cells has clear implications for the underlying circuitry. Our previous recordings from the smooth GABAergic neurones indicated that they have the normal range of orientation selectivity. Thus, assuming the smooth neurones are inhibitory, many with different orientation tunings must provide a convergent input to cortical neurones. Obviously, the net effect on a particular neurone can come from both presynaptic and postsynaptic influences and the relative balance between these two may be the underlying difference between those neurones showing a distinct hyperpolarization and those that do not.

The striking observation was that for all the stimulus conditions used, many of the inhibitory events that were suggested previously on the basis of extracellular recording were not apparent in the intracellular records. We pursue the implications of this finding in the following papers (Berman *et al.* 1991; Dehay, Douglas, Martin & Nelson, 1991; Douglas & Martin, 1991).

We thank John Anderson for expert technical support and Dr S. J. Thomas for excellent assistance. We are indebted to the Wellcome Trust for support. R.J.D. was supported by the Medical Research Council (South Africa). K.A.C.M. is the Henry Head Research Fellow of the Royal Society.

REFERENCES

ALBUS, K. (1980). The detection of movement direction and the effects of contrast reversal in the cat's striate cortex. *Vision Research* **20**, 289–293.

BARLOW, H. B. (1981). The Ferrier Lecture. Critical limiting factors in the design of the eye and visual cortex. *Proceedings of the Royal Society* B **212**, 1–34.

BARLOW, H. B. & LEVICK, W. R. (1965). The mechanism of directionally selective units in rabbit's retina. *Journal of Physiology* **178**, 477–504.

BENEVENTO, L. A., CREUTZFELDT, O. D. & KUHNT, U. (1972). Significance of intracortical inhibition. *Nature* **283**, 124–126.

BERMAN, N. J., BUSH, P. C. & DOUGLAS, R. J. (1989). Adaptation and bursting may be controlled by a single fast potassium current. *Quarterly Journal of Experimental Physiology* **74**, 223–226.

BERMAN, N. J., DOUGLAS, R. J., MARTIN, K. A. C. & WHITTERIDGE, D. (1991). Mechanisms of inhibition in cat visual cortex. *Journal of Physiology* **440**, 697–722.

BISHOP, P. O., COOMBS, J. S. & HENRY, G. H. (1971). Interaction effects of visual contours on the discharge frequency of simple striate neurones. *Journal of Physiology* **219**, 659–687.

BISHOP, P. O., COOMBS, J. S. & HENRY, G. H. (1973). Receptive fields of simple cells in the cat striate cortex. *Journal of Physiology* **231**, 31–60.

BISHOP, P. O., KATO, H. & ORBAN, G. A. (1980). Direction-selective cells in complex family in cat striate cortex. *Journal of Neurophysiology* **43**, 1266–1283.

BOLZ, J. & GILBERT, C. D. (1986). Generation of end-inhibition in the visual cortex via interlaminar connections. *Nature* **320**, 362–365.

BONDS, A. B. (1989). Role of inhibition in the specification of orientation selectivity of cells in the cat striate cortex. *Visual Neuroscience* **2**, 41–55.

BULLIER, J. & HENRY, G. H. (1979). Ordinal position of neurons in cat striate cortex. *Journal of Neurophysiology* **42**, 1251–1263.

BURR, D., MORRONE, C. & MAFFEI, L. (1981). Intra-cortical inhibition prevents simple cells from responding to textured visual patterns. *Experimental Brain Research* **43**, 455–458.

CONNORS, B. W., GUTNICK, M. J. & PRINCE, D. A. (1982). Electrophysiological properties of neocortical neurons *in vitro*. *Journal of Neurophysiology* **48**, 1302–1320.

CREUTZFELDT, O. D., KUHNT, U. & BENEVENTO, L. A. (1974). An intracellular analysis of visual cortical neurones to moving stimuli: responses to a co-operative neuronal network. *Experimental Brain Research* **21**, 251–274.

DEAN, A. F., HESS, R. F. & TOLHURST, D. J. (1980). Divisive inhibition involved in direction selectivity. *Journal of Physiology* **308**, 84–85*P*.

DEHAY, C., DOUGLAS, R. J., MARTIN, K. A. C. & NELSON, C. (1991). Excitation by geniculocortical synapses is not 'vetoed' at the level of dendritic spines in cat visual cortex. *Journal of Physiology* **440**, 723–734.

DEVALOIS, R. L., YUND, E. W. & HEPLER, N. (1982). The orientation and direction selectivity of cell in macaque visual cortex. *Vision Research* **22**, 531–544.

DOUGLAS, R. J. & MARTIN, K. A. C. (1987). A multiprocessor system for presenting visual stimuli and logging extra- and intracellular neuronal responses. *Journal of Physiology* **394**, 12*P*.

DOUGLAS, R. J. & MARTIN, K. A. C. (1990). Neocortex. In *Synaptic Organisation of the Brain*, ed. SHEPHERD, G., pp. 220–248. Oxford University Press, New York.

DOUGLAS, R. J. & MARTIN, K. A. C. (1991). A functional microcircuit for cat visual cortex. *Journal of Physiology* **440**, 735–768.

DOUGLAS, R. J., MARTIN, K. A. C. & WHITTERIDGE, D. (1987). Estimation of the amplitudes of theoretical unitary excitatory post-synaptic potentials in neurones of the cat striate cortex by a combination of biophysical and anatomical measurement. *Journal of Physiology* **394**, 110*P*.

DREIFUSS, J. J., KELLY, J. S. & KRNJEVIĆ, K. (1969). Cortical inhibition and gamma-aminobutyric acid. *Experimental Brain Research* **9**, 137–154.

DUYSENS, J. & ORBAN, G. A. (1981). Is stimulus movement of particular importance in the functioning of cat visual cortex? *Brain Research* **220**, 184–187.

EMERSON, R. C., CITRON, M. C., FELLEMAN, D. J. & KAAS, J. H. (1985). A proposed mechanism and site for cortical direction selectivity. In *Models of the Visual Cortex*, ed. ROSE, D. R. & DOBSON, V. G., pp. 420–431. John Wiley & Sons, Chichester, New York.

EMERSON, R. C. & COLEMAN, L. (1981). Does image movement have a special nature for neurons in the cat's striate cortex? *Investigative Ophthalmology and Visual Science* **20**, 766–783.

EMERSON, R. C. & GERSTEIN, G. L. (1977*a*). Simple striate neurons in the cat. I. Comparison of responses to moving and stationary stimuli. *Journal of Neurophysiology* **40**, 119–135.

EMERSON, R. C. & GERSTEIN, G. L. (1977*b*). Simple striate neurons in the cat. II. Mechanisms underlying directional asymmetry and direction selectivity. *Journal of Neurophysiology* **40**, 136–155.

EYSEL, U. TH., MUCHE, T. & WÖRGÖTTER, F. (1988). Lateral interactions at direction-selective striate neurones in the cat demonstrated by local cortical inactivation. *Journal of Physiology* **399**, 657–675.

FERSTER, D. (1981). A comparison of binocular depth mechanisms in areas 17 and 18 of the cat visual cortex. *Journal of Physiology* **311**, 623–655.

FERSTER, D. (1986). Orientation selectivity of synaptic potentials in neurons of cat primary visual cortex. *Journal of Neuroscience* **6**, 1284–1301.

FERSTER, D. (1987). Origin of orientation-selective EPSPs in simple cells of cat visual cortex. *Journal of Neuroscience* **7**, 1780–1791.

FERSTER, D. (1988). Spatially opponent excitation and inhibition in simple cells of the cat visual cortex. *Journal of Neuroscience* **8**, 1172–1180.

FERSTER, D. & LINDSTRÖM, S. (1983). An intracellular analysis of geniculo-cortical connectivity in area 17 of the cat. *Journal of Physiology* **342**, 181–215.

GANZ, L. & FELDER, R. (1984). Mechanism of directional selectivity in simple neurons of the cat's visual cortex analyzed with stationary flash sequences. *Journal of Neurophysiology* **51**, 294–324.

GILBERT, C. D. (1977). Laminar differences in receptive field properties of cells in cat primary visual cortex. *Journal of Physiology* **268**, 391–421.

GILBERT, C. D. (1983). Microcircuitry of cat visual cortex. *Annual Review of Neuroscience* **6**, 217–247.

GOODWIN, A. W., HENRY, G. H. & BISHOP, P. O. (1975). Direction selectivity in simple striate cells: properties and mechanism. *Journal of Neurophysiology* **38**, 1500–1523.

HAMMOND, P. & MACKAY, D. M. (1977). Differential responsiveness of simple and complex cells in cat striate cortex to visual texture. *Experimental Brain Research* **30**, 275–296.

HEGGELUND, P. (1981*a*). Receptive field organization of simple cells in cat striate cortex. *Experimental Brain Research* **42**, 89–98.

HEGGELUND, P. (1981*b*). Receptive field organization of complex cells in cat striate cortex. *Experimental Brain Research* **42**, 99–107.

HENRY, G. H. (1977). Receptive field classes of cells in the striate cortex of the cat. *Brain Research* **133**, 1–28.

HENRY, G. H., HARVEY, A. R. & LUND, J. S. (1979). The afferent connections and laminar distribution of cells in the cat striate cortex. *Journal of Comparative Neurology* **187**, 725–744.

HESS, R. & MURATA, K. (1974). Effects of glutamate and GABA on specific response properties of neurones in visual cortex. *Experimental Brain Research* **21**, 285–297.

HOFFMAN, K.-P. & STONE, J. (1971). Conduction velocity of afferents to cat visual cortex: a correlation with cortical receptive field properties. *Brain Research* **32**, 460–466.

HUBEL, D. H. & WIESEL, T. N. (1959). Receptive fields of single neurones in the cat's striate cortex. *Journal of Physiology* **148**, 574–591.

HUBEL, D. H. & WIESEL, T. N. (1962). Receptive fields, binocular interaction and functional architecture in the cat's visual cortex. *Journal of Physiology* **160**, 106–154.

HUBEL, D. H. & WIESEL, T. N. (1965). Receptive fields and functional architecture in two non-striate visual areas (18 and 19) of the cat. *Journal of Neurophysiology* **28**, 229–289.

INNOCENTI, G. M. & FIORE, L. (1974). Post-synaptic inhibitory components of the responses to moving stimuli in area 17. *Brain Research* **80**, 122–126.

KOCH, C., DOUGLAS, R. J. & WEHMEIER, U. (1990). Visibility of synaptically induced conductance changes: theory and simulations of anatomically characterized cortical pyramidal cells. *Journal of Neuroscience* **10**, 1728–1744.

KOCH, C. & POGGIO, T. (1985). The synaptic veto mechanism: does it underlie direction and orientation selectivity in the visual cortex? In *Models of the Visual Cortex*, ed. ROSE, D. & DOBSON, V. G., pp. 408–419. John Wiley & Sons, Chichester, New York.

LUND, J. S. (1988). Anatomical organization of macaque monkey striate visual cortex. *Annual Review of Neuroscience* **11**, 253–288.

MARTIN, K. A. C. (1984). Neuronal circuits in cat striate cortex. In *Cerebral Cortex*, vol. 2,

Functional Properties of Cortical Cells, ed. JONES, E. G. & PETERS, A., pp. 241–284. Plenum Press, New York.

MARTIN, K. A. C. (1988). The Wellcome Prize Lecture. From single cells to simple circuits in the cerebral cortex. *Quarterly Journal of Experimental Physiology* **73**, 637–702.

MARTIN, K. A. C. & WHITTERIDGE, D. (1984). Form, function and intracortical projections of spiny neurones in the striate visual cortex of the cat. *Journal of Physiology* **353**, 463–504.

MOVSHON, J. A., THOMPSON, I. D. & TOLHURST, D. J. (1978*a*). Spatial summation in the receptive fields of simple cells in the cat's striate cortex. *Journal of Physiology* **283**, 53–77.

MOVSHON, J. A., THOMPSON, I. D. & TOLHURST, D. J. (1978*b*). Receptive field organization of complex cells in the cat's striate cortex. *Journal of Physiology* **283**, 79–99.

NELSON, J. I. & FROST, B. J. (1978). Orientation-selective inhibition from beyond the classic visual receptive field. *Brain Research* **139**, 359–364.

ORBAN, G. A. (1984). *Neuronal Operations in the Visual Cortex*. Springer Verlag, Berlin, Heidelberg.

PALMER, L. A. & DAVIS, T. L. (1981*a*). Receptive field structure in cat striate cortex. *Journal of Neurophysiology* **46**, 260–276.

PALMER, L. A. & DAVIS, T. L. (1981*b*). Comparison of responses to moving and stationary stimuli in cat striate cortex. *Journal of Neurophysiology* **46**, 277–295.

PERRY, V. H. & LINDEN, R. (1982). Evidence for dendritic competition in the developing retina. *Nature* **297**, 683–685.

PURVES, R. D. (1981). *Microelectrode Methods for Intracellular Recording and Ionophoresis*. Academic Press, London.

RAMOA, A. S., SHADLEN, M., SKOTTUN, B. C. & FREEMAN, R. D. (1986). A comparison of inhibition in orientation and spatial frequency selectivity of cat visual cortex. *Nature* **321**, 237–239.

SCHWINDT, P. C., SPAIN, W. J., FOEHRING, R. C., CHUBB, M. C. & CRILL, W. E. (1988). Slow conductances in neurons from cat sensorimotor cortex *in vitro* and their role in slow excitability changes. *Journal of Neurophysiology* **59**, 450–467.

SILLITO, A. M. (1975). The effectiveness of bicuculline as an antagonist of GABA and visually evoked inhibition in the cat's striate cortex. *Journal of Physiology* **250**, 287–304.

SILLITO, A. M. (1977). Inhibitory processes underlying direction specificity of simple, complex and hypercomplex cells in the cat's visual cortex. *Journal of Physiology* **271**, 299–720.

SILLITO, A. M. (1979). Inhibitory mechanisms influencing complex cell orientation selectivity and their modification at high resting discharge levels. *Journal of Physiology* **289**, 33–53.

SILLITO, A. M. (1984). Functional considerations of the operation of GABAergic inhibitory processes in the visual cortex. In *Cerebral Cortex*, vol. 2, *Functional Properties of Cortical Cells*, ed. JONES, E. G. & PETERS, A., pp. 91–117. Plenum Press, New York.

TOYAMA, K., KIMURA, M. & TANAKA, K. (1981). Cross-correlation analysis of interneural activity in cat visual cortex. *Journal of Neurophysiology* **46**, 191–201.

TS'O, D. Y., GILBERT, C. D. & WIESEL, T. N. (1986). Relationships between horizontal interactions and functional architecture as revealed by cross correlation analysis. *Journal of Neuroscience* **6**, 1160–1170.

TSUMOTO, T., ECKART, W. & CREUTZFELDT, O. D. (1979). Modification of orientation sensitivity of cat visual cortex neurons by removal of GABA-mediated inhibition. *Experimental Brain Research* **34**, 351–363.

WHITE, E. L. (1989). *Cortical Circuits*. Birkhauser, Boston.